



BERKELEY LAB

Bringing Science Solutions to the World



**NC STATE
UNIVERSITY**



Brookhaven
National Laboratory



U.S. DEPARTMENT OF
ENERGY

Office of Science

The Progress of Silicon Carbide Low Gain Avalanche Diodes (SiC LGADs)

Tao Yang¹, Ben Sekely², Yashas Satapathy², Greg Allion², Gil Atar², Philip Barletta², Carl Haber¹,
Steve Holland¹, John Muth², Spyridon Pavlidis², Stefania Stucci³, Abraham Tishelman³

¹ Lawrence Berkeley National Laboratory

² North Carolina State University

³ Brookhaven National Laboratory

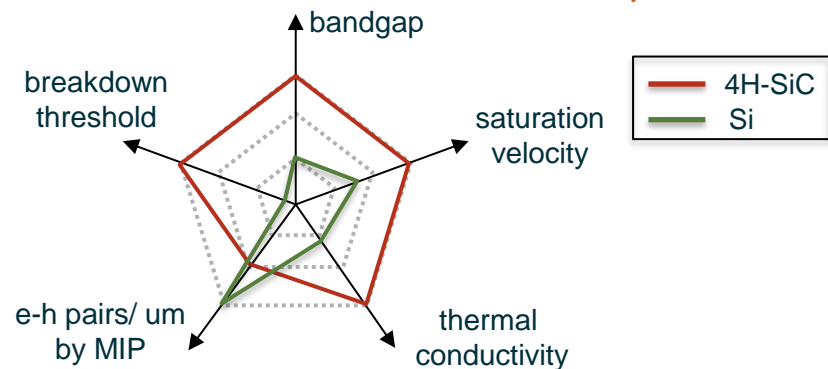
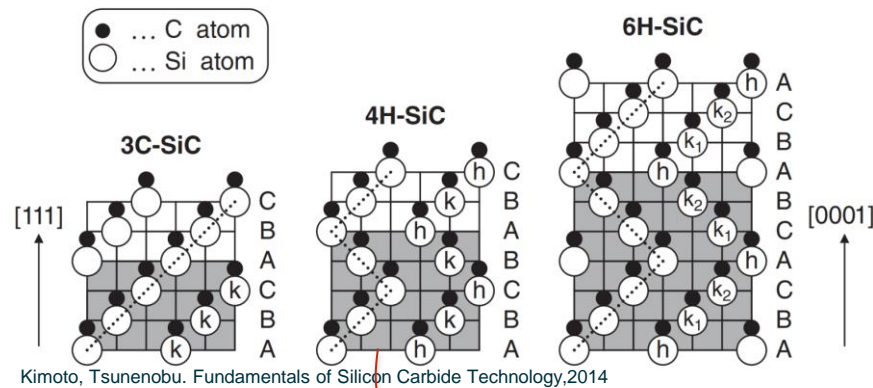
Coordinating Panel for Advanced Detectors (CPAD) Workshop, 2024, Knoxville

2024-11-20

Silicon Carbide for Charged Particle Detection

As a wide-band semiconductor material, among many silicon carbide (SiC) polymorphs, 4H-SiC has potential applications in radiation detection, especially **fast time detection** and **high temperature environment**.

Schematic structures of popular SiC polytypes: 3C, 4H and 6H



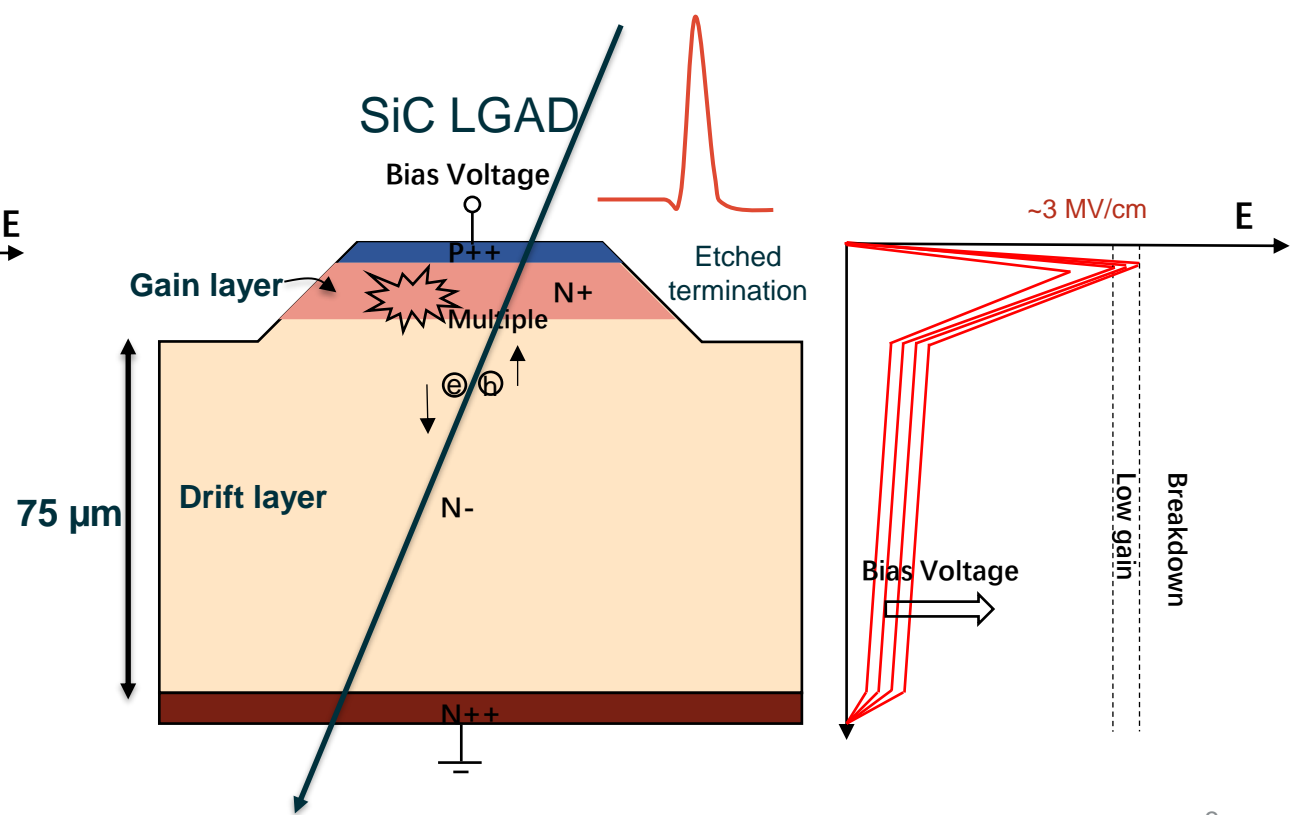
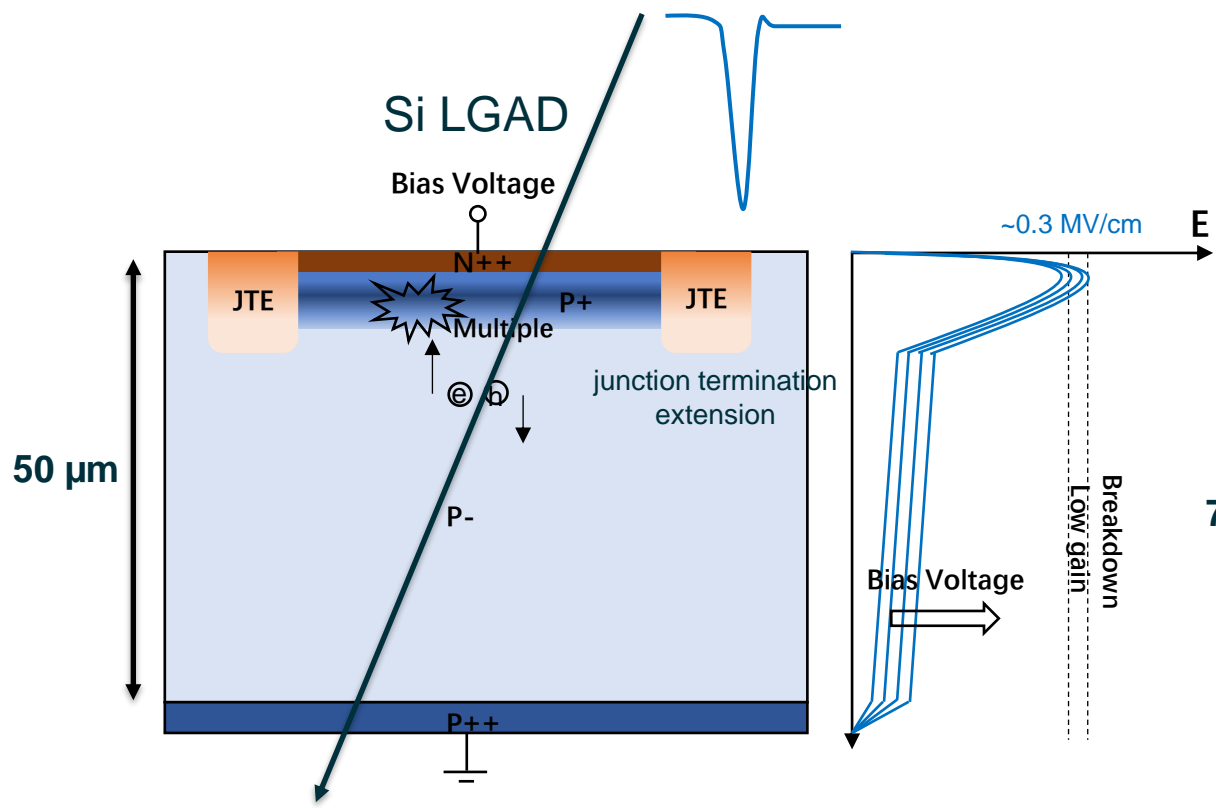
The parameters of Si and 4H-SiC

Parameters	Si	4H-SiC
Band gap[eV]	1.12	3.26
Relative permittivity	11.7	9.76
Thermal conductivity[W/K·cm]	1.5	4.9
Average ionization energy [eV/e-h pair]	3.6	5-9
Average e-h pairs for MIP [μm^{-1}]	~78	~55
Breakdown Threshold [MV/cm]	~0.3	~2.0
Atom displacement energy [eV]	13-15	30-40
Funno factor	0.11-0.13	0.04-0.12
Electron mobility [cm^2/Vs]	1450	800
Hole mobility [cm^2/Vs]	450	115
Electron saturation velocity [cm/s]	1×10^7	2×10^7
Hole saturation velocity [cm/s]	0.6×10^7	1.8×10^7

Silicon Carbide Low Gain Avalanche Detector (SiC LGAD)

- 50 μm P-type ($\sim 1\text{e}13 \text{ cm}^{-3}$) drift layer
- Primary electrons multiplication.
- Ion implantation for gain layer and JTE
- Electric field: $\sim 0.3 \text{ MV/cm}$
- Gain layer doping: $\sim 1\text{e}16 \text{ cm}^{-3}$

- 75 μm N-type drift layer ($\sim 2\text{e}14 \text{ cm}^{-3}$)
- Primary holes multiplication.
- Epitaxial stack with etched termination (or ion implantation)
- Electric field: $\sim 3 \text{ MV/cm}$
- Gain layer doping: $> 2\text{e}17 \text{ cm}^{-3}$



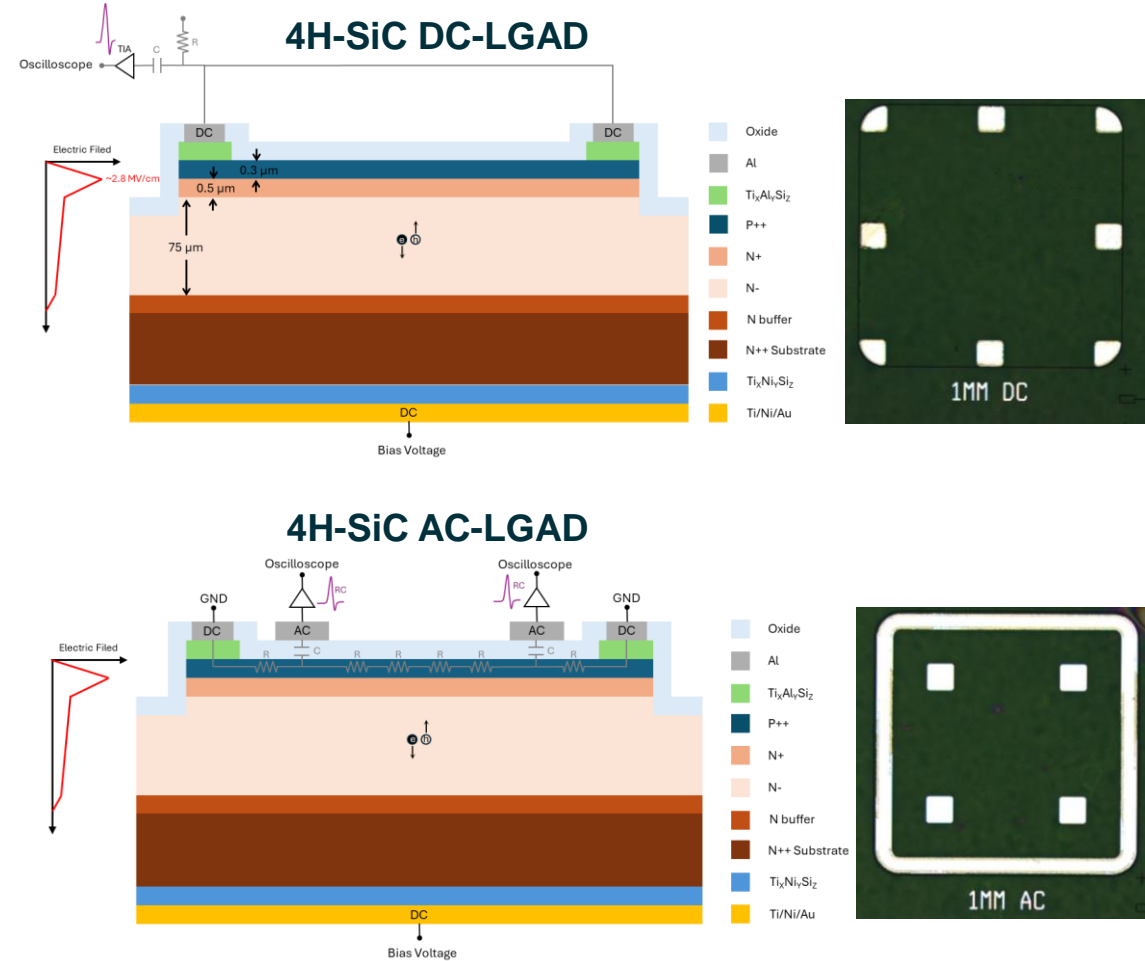
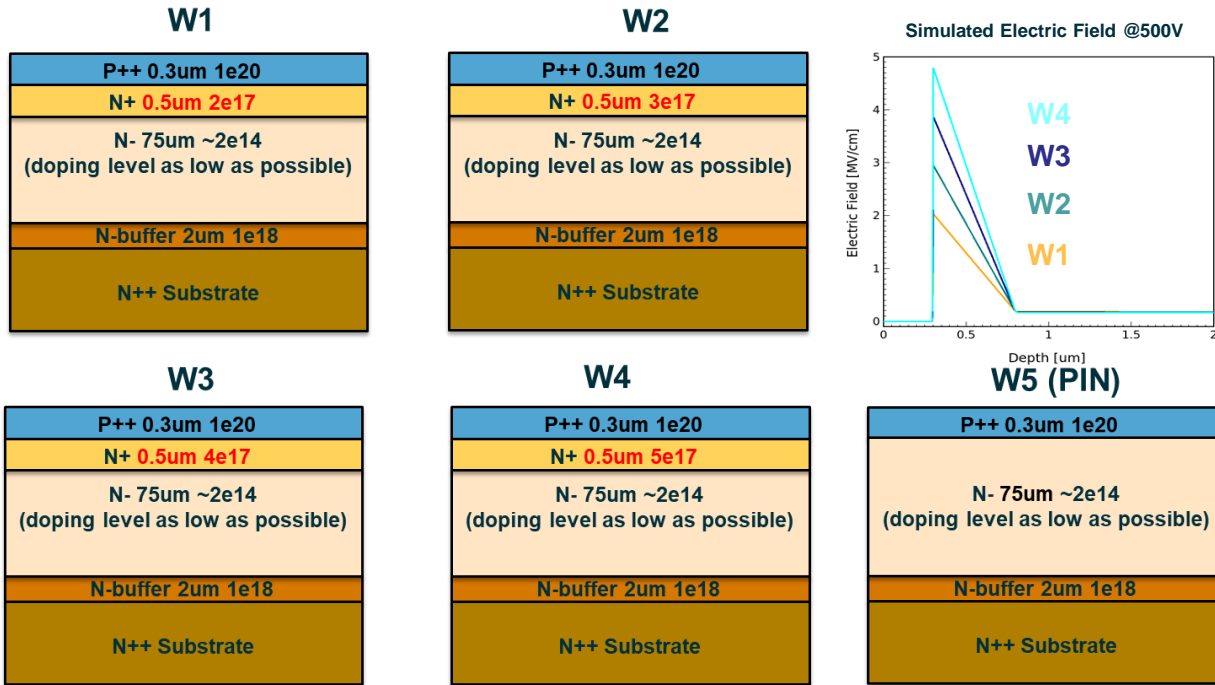
The Design & Fabrication of 4H-SiC LGAD by LBNL and NCSU

Based on 4H-SiC wafers with custom epitaxial stacks

- 0.5 μm Gain layer with doping concentration from $2\text{e}17\text{ cm}^{-3}$ to $5\text{e}17\text{ cm}^{-3}$, that target the electric field between 2 MV/cm to 5 MV/cm .
- Wide doping density range ensure coverage of a wide breakdown voltage range while accounting for the fluctuations of epitaxial growth.
- Etched-Termination isolates the segmented devices.

More fabrication details on:
 B.Sekely et al., "Progress Towards 4H-SiC Low Gain Avalanche Detectors (LGADs)," in Book of Abstracts from the ICSCRM 2024, pp.694-223695, Sept 2024.
 doi:10.4028/b-f6NMEP.224

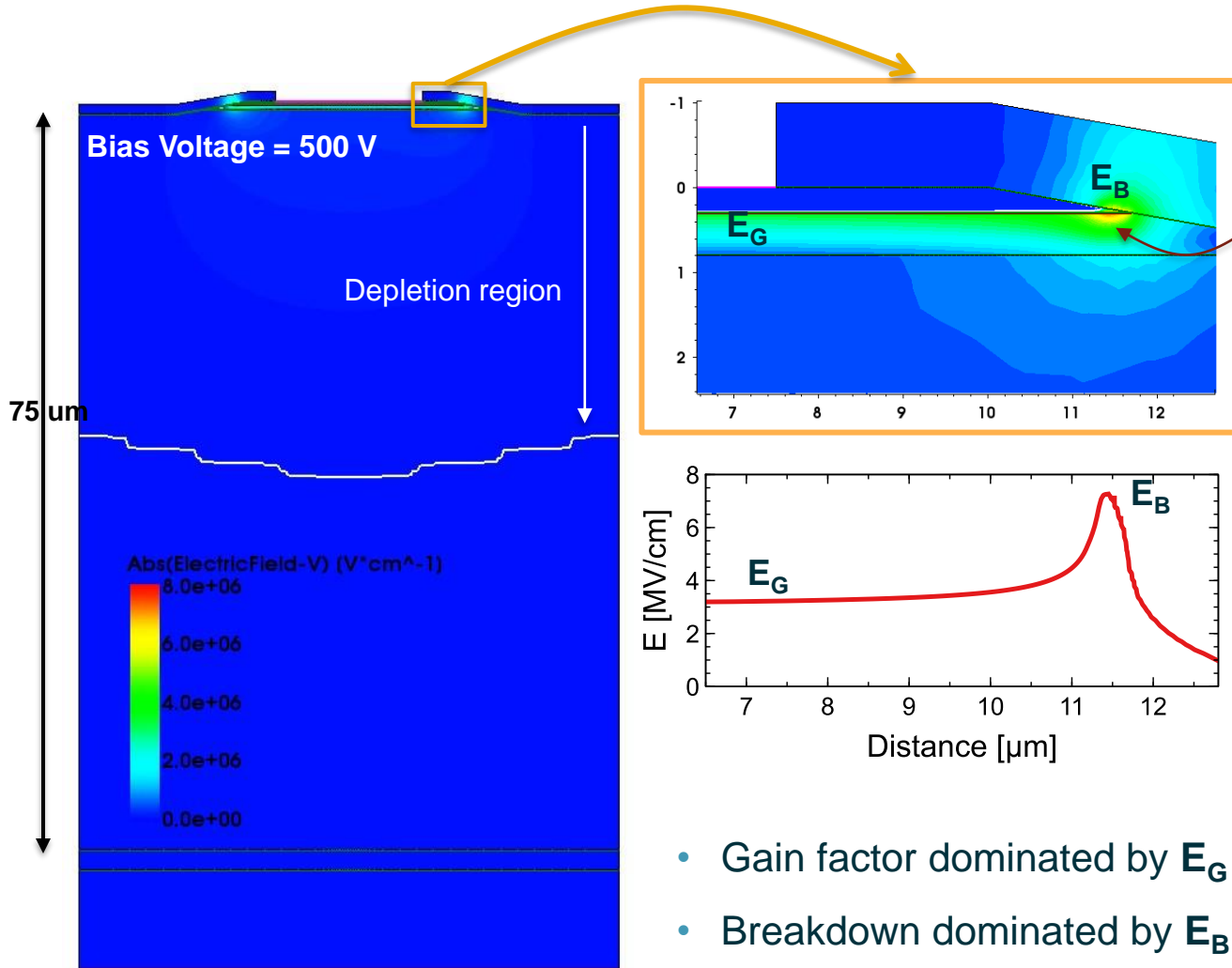
Custom Epitaxial Wafers



Issue of 4H-SiC LGAD with Bevel-Etched Termination

The bevel-etched 4H-SiC LGADs currently have to adopt a **negative bevel-etched angle**, which increases the junction electric field on the surface of bevel, leading to a reduction in the breakdown voltage of the device.

(See p22~p23 on backup)



- 1) The electric field peak E_B appears close to the bevel surface.
- 2) High bias voltage (~1000 V) should be applied to deplete N-type drift layer($d=75\mu\text{m}$, $N_{\text{eff}}=2\text{e}14 \text{ cm}^{-3}$)

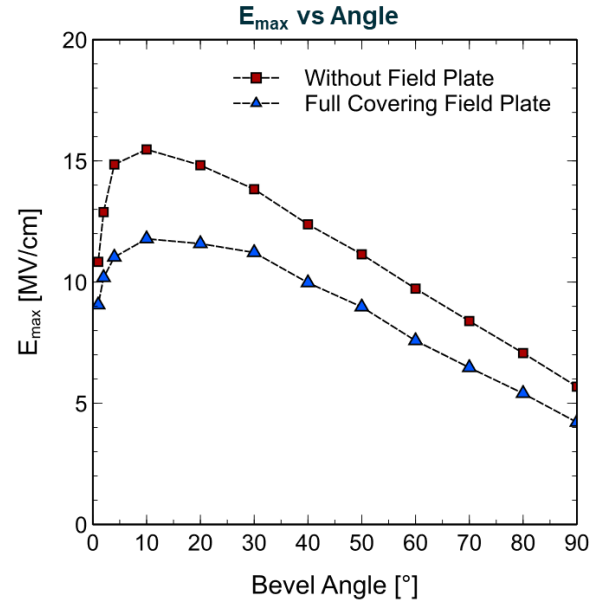
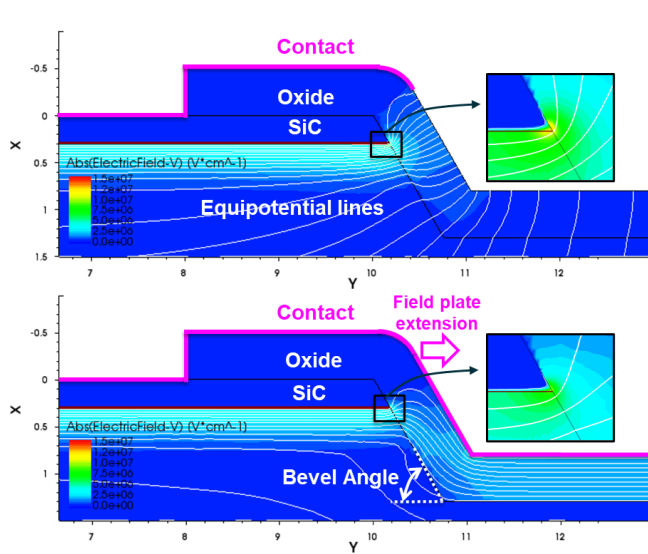
breakdown here 😞

$$V_{\text{dep}} = \frac{q|N_{\text{eff}}|d^2}{2\epsilon\epsilon_0}$$

- 3) The E_B exceeds the breakdown threshold easily when the bias voltage increase, that caused the device **breakdown before full depletion** – **early breakdown**.

- Gain factor dominated by E_G
- Breakdown dominated by E_B

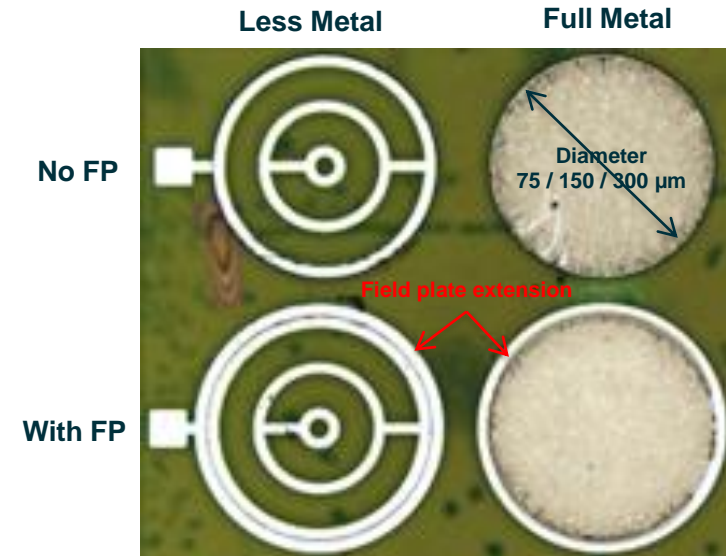
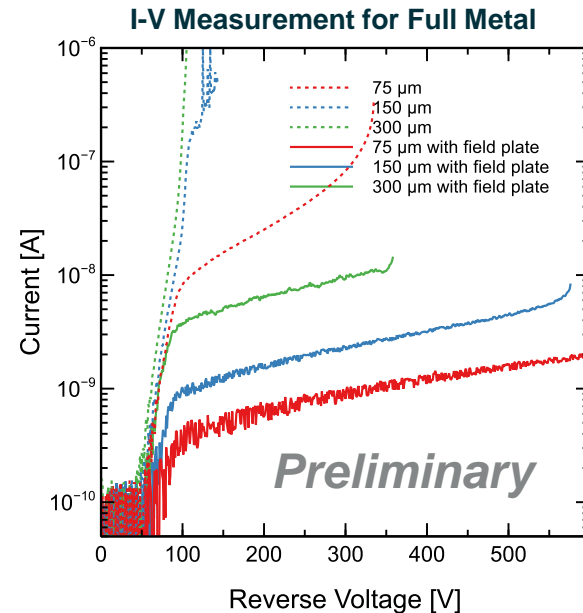
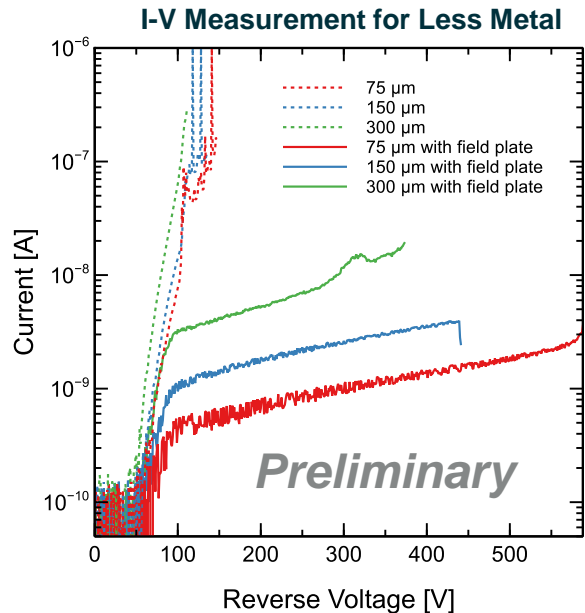
The Effects of Field Plate



Higher breakdown voltage by lower electric field peak at bevel with field plate.

- Based on the TCAD simulation, the equipotential lines are reformed to parallel with the surface by the extended field plate. Then the electric field is suppressed.
- Observed higher breakdown voltage for the devices with field plate.

Field plate can effectively increase breakdown voltage

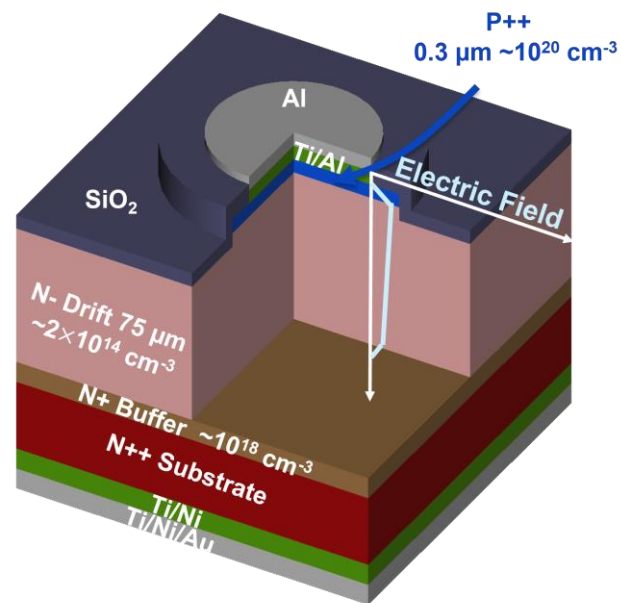


I-V & C-V Comparison of PIN and LGAD

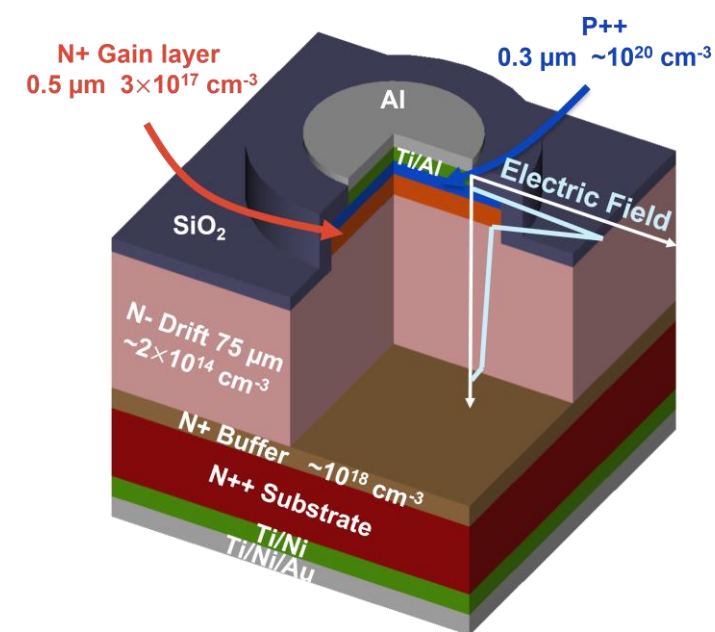
- The wafer (W2) with 4H-SiC epitaxial stacks having specific doping concentrations, which exhibit the typical electric field distribution of LGADs.
- For comparison, the wafer (W5) is without gain layer, resulting in a typical PIN electric field distribution.
- The measurements:
 - Both LGAD and PIN have high breakdown voltages.
 - Lower breakdown voltage and higher leakage current of LGAD are observed comparing PIN

More details on:
T. Yang et al., "Characterization of 4H-SiC Low Gain Avalanche Detectors (LGADs)," 2024

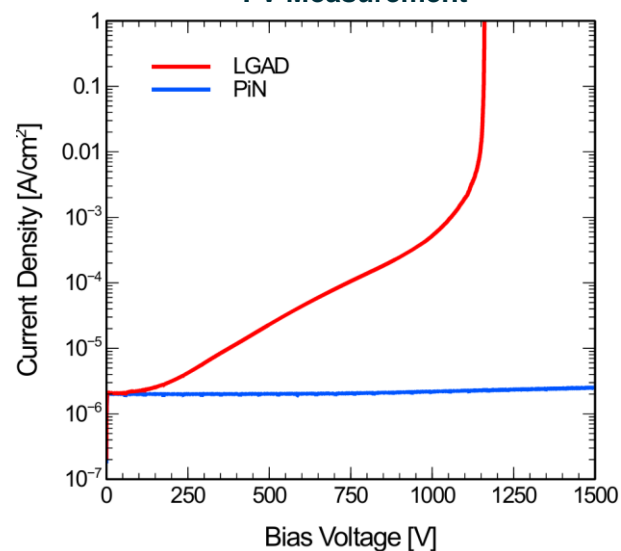
4H-SiC PIN (W5)



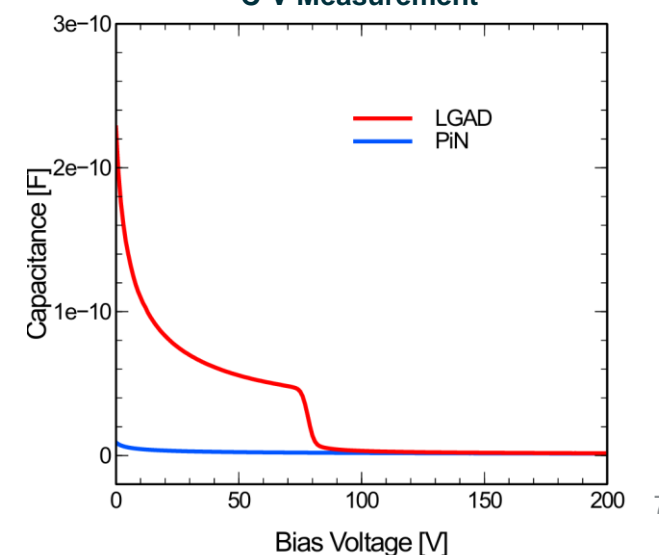
4H-SiC LGAD (W2)



I-V Measurement



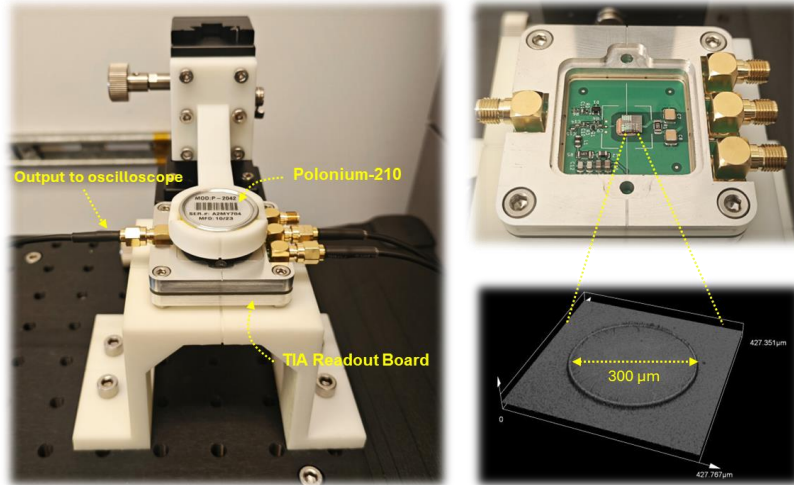
C-V Measurement



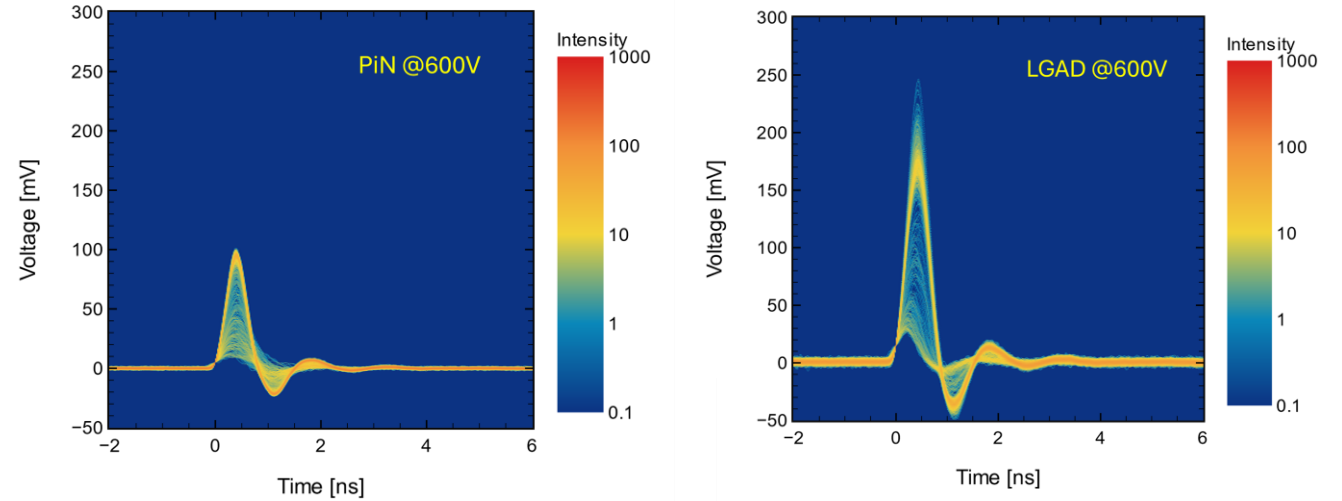
Response of α particles from ^{210}Po Source

✓ Evidence of the low gain carrier multiplication

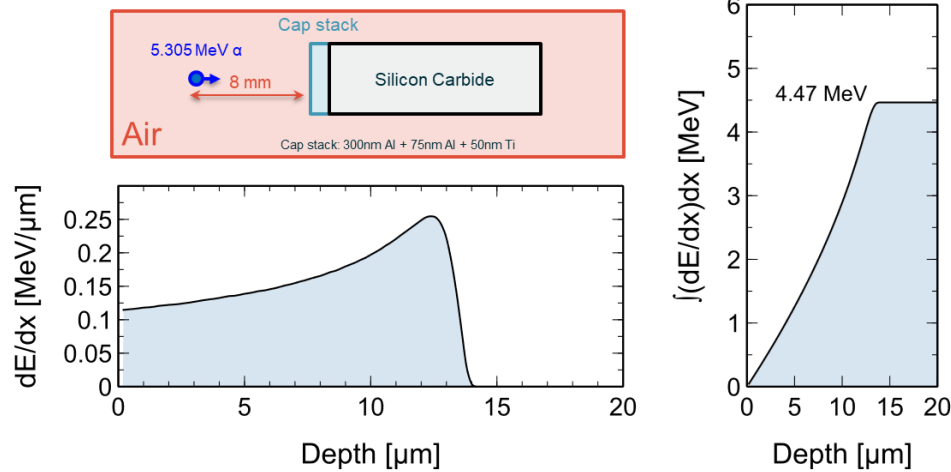
Test Setup



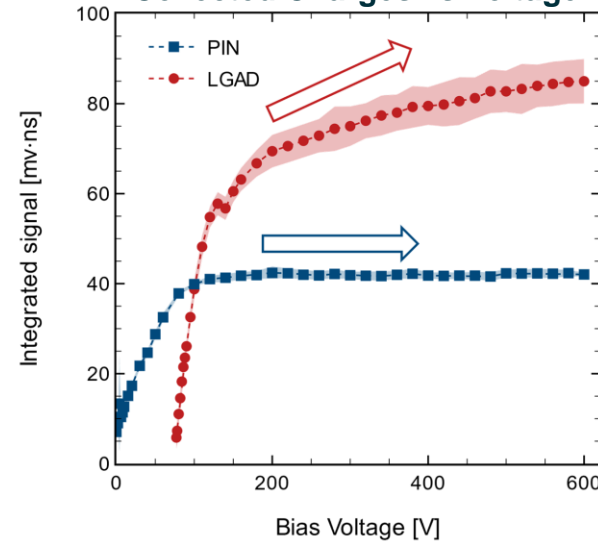
Signal pulses from α particles



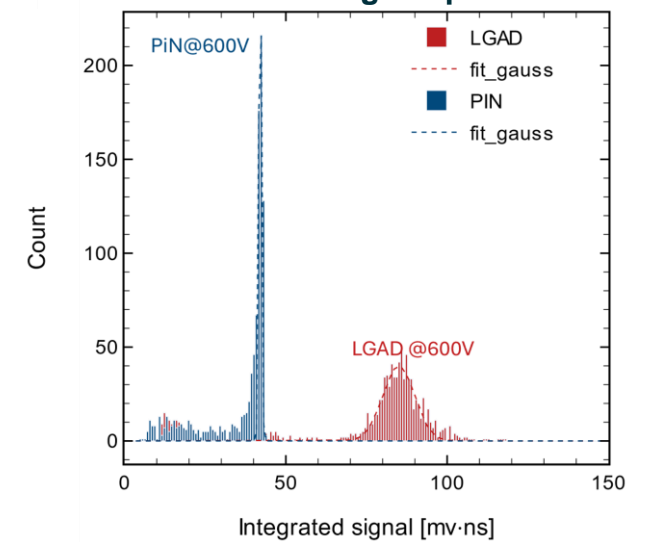
SRIM Simulation



Collected Charges vs Voltage

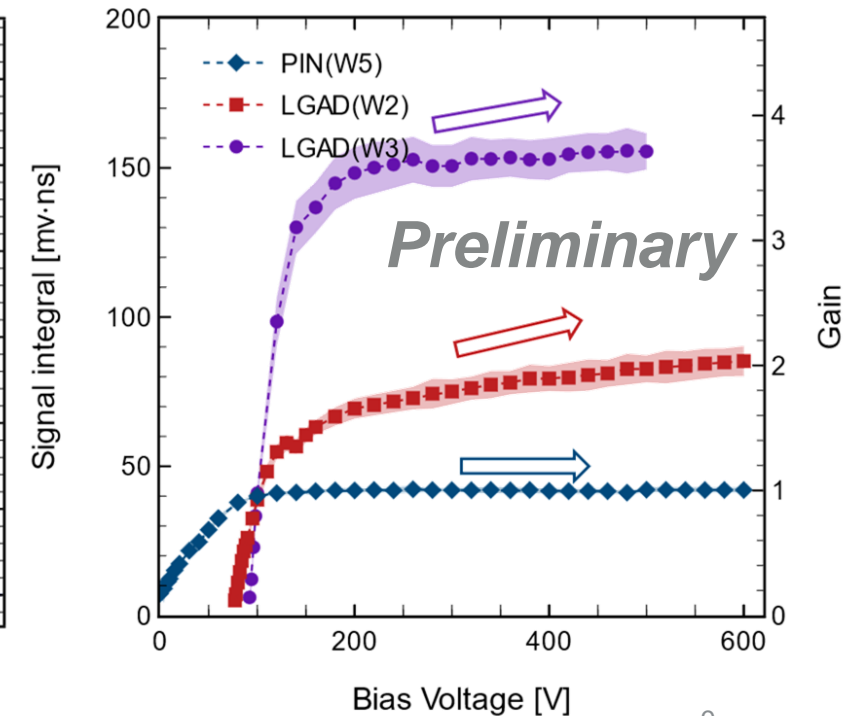
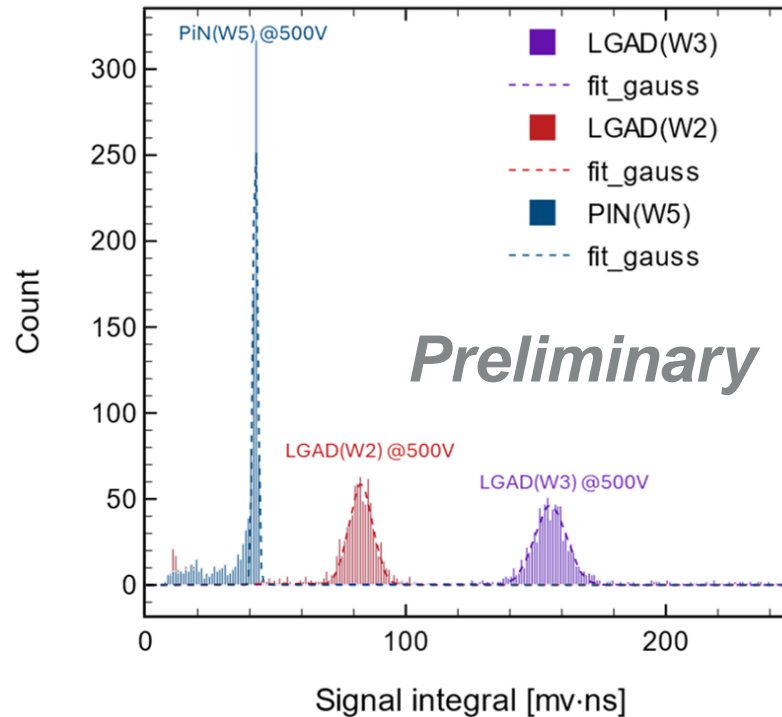
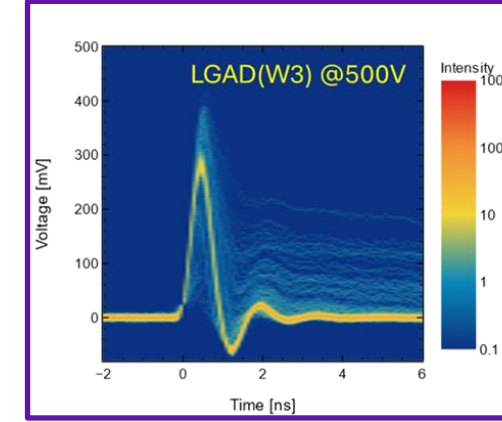
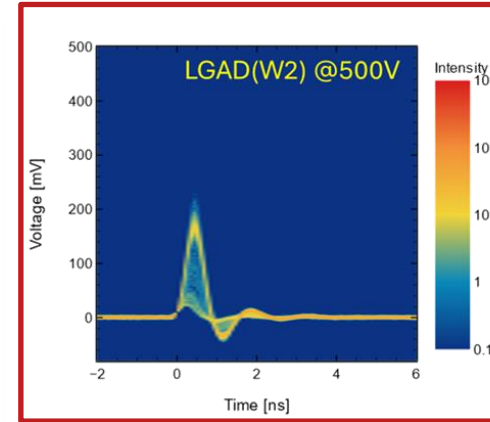
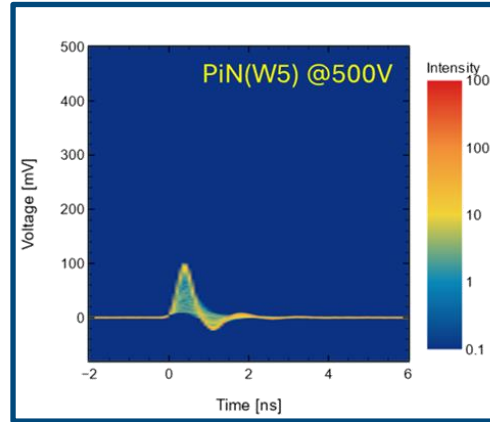


Collected Charges Spectrum



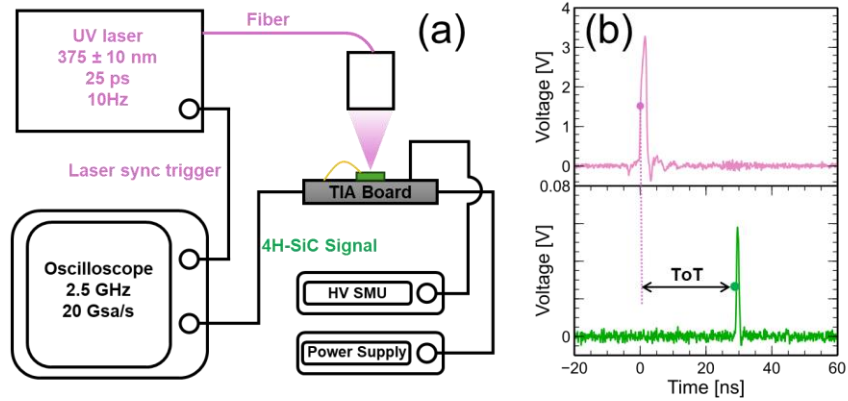
Response of α particles for Different Gain layer Doping Concentration

- As expected, a higher doping concentration of the gain layer has a larger gain at the same voltage.
- The collected charge of the LGAD increases with voltage, but not very fast. In the higher gain of W3, the gain changes slowly with increasing voltage.
- Higher gain exhibits greater multiplication randomness, resulting in a wider charge collection distribution.

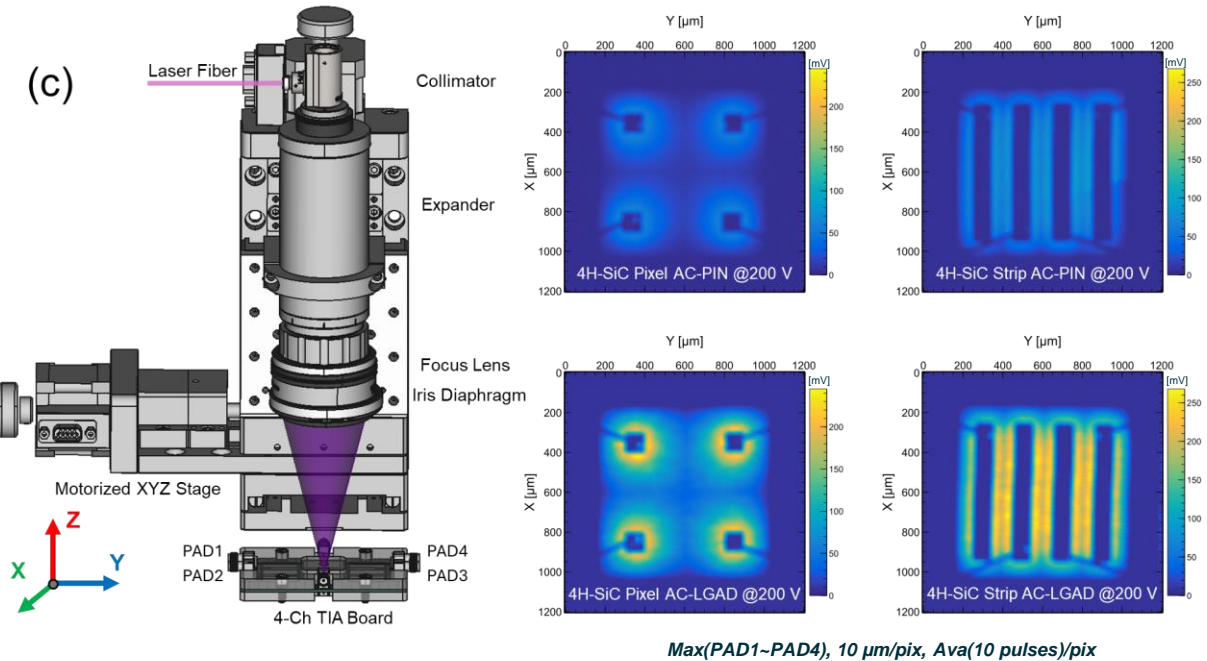
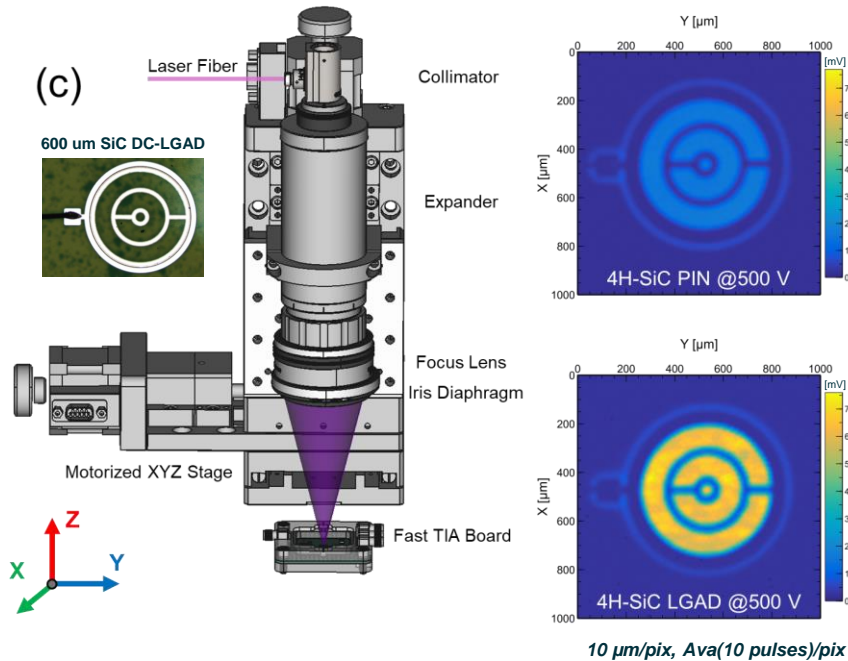
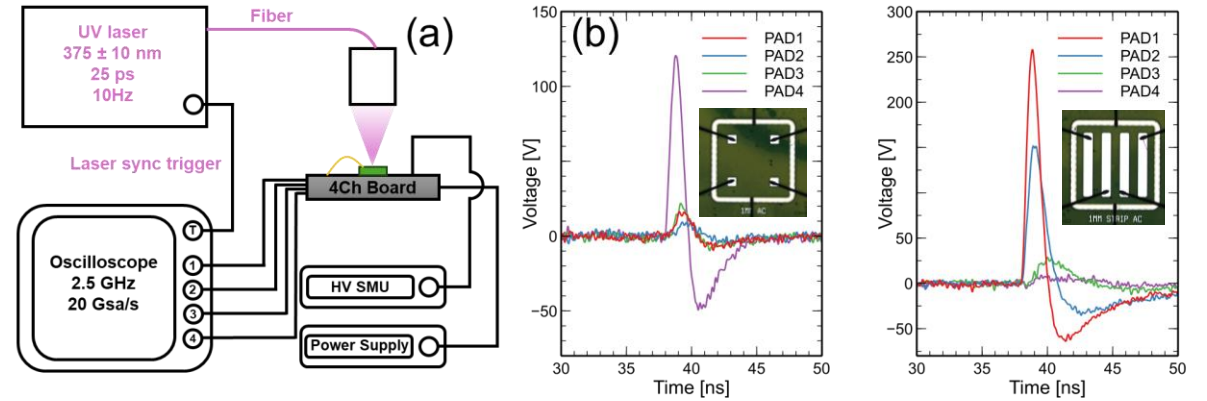


Ultraviolet Transient Current Technique (UV-TCT)

Single Channel for SiC DC-LGAD / PIN

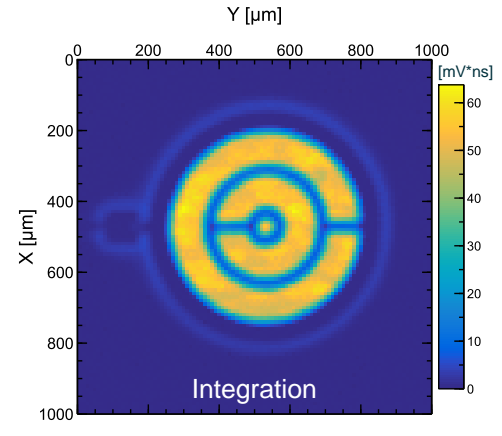
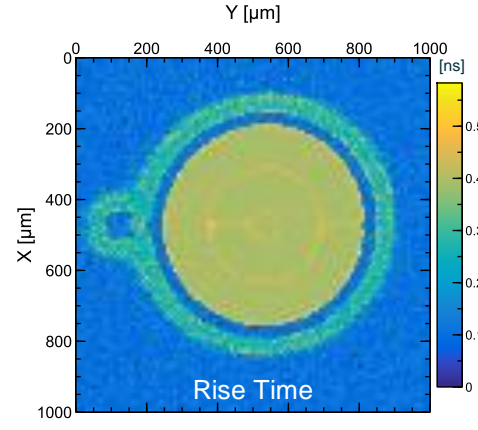
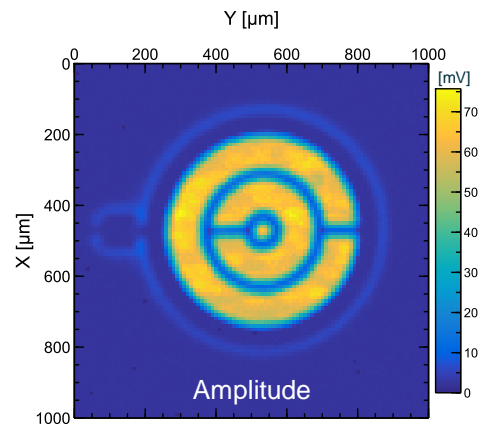
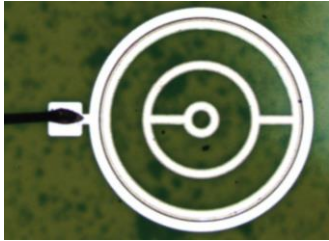


Four Channels for SiC AC-LGAD / PIN

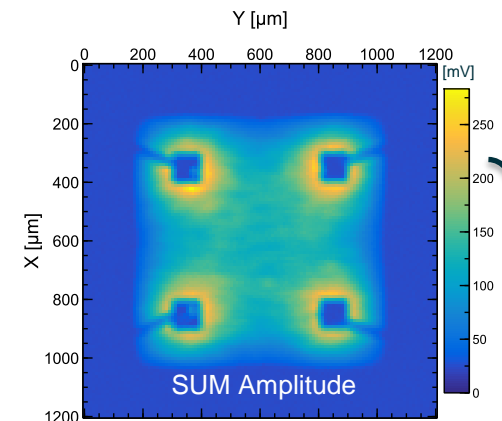
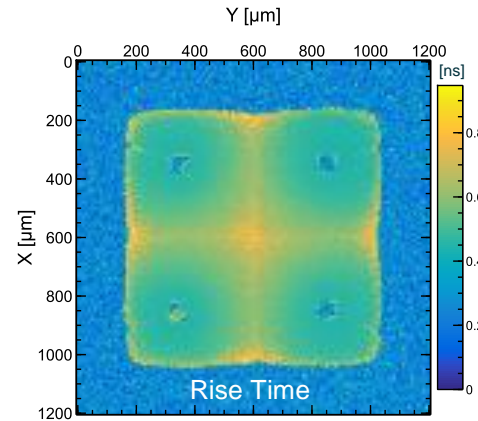
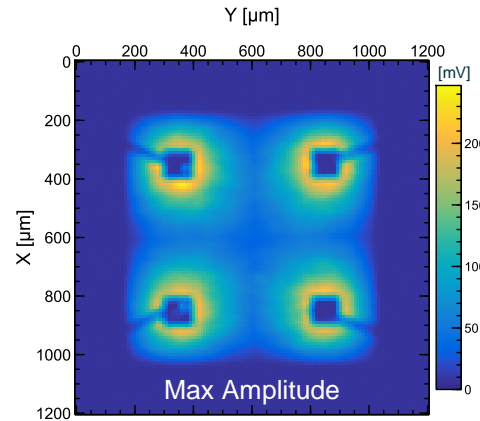
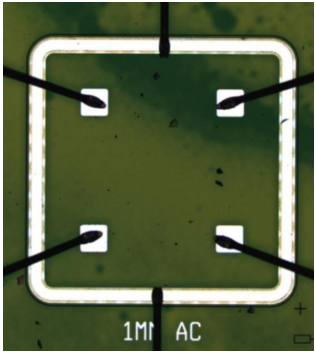


Scanning Results by UV-TCT

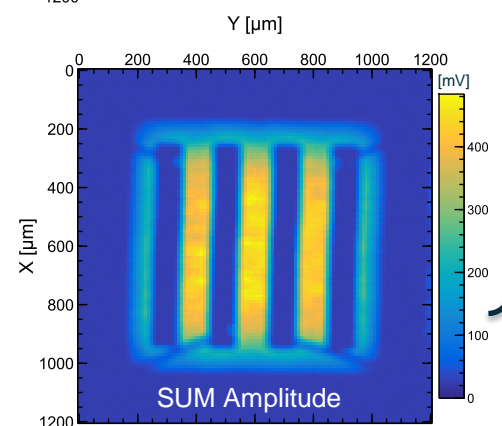
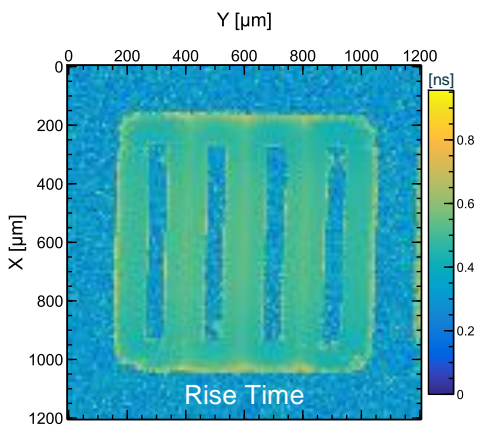
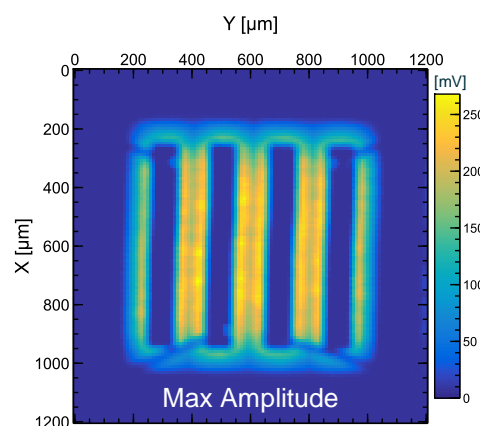
600 μm SiC DC-LGAD



1mm SiC Pixel AC-LGAD



1mm SiC Strip AC-LGAD



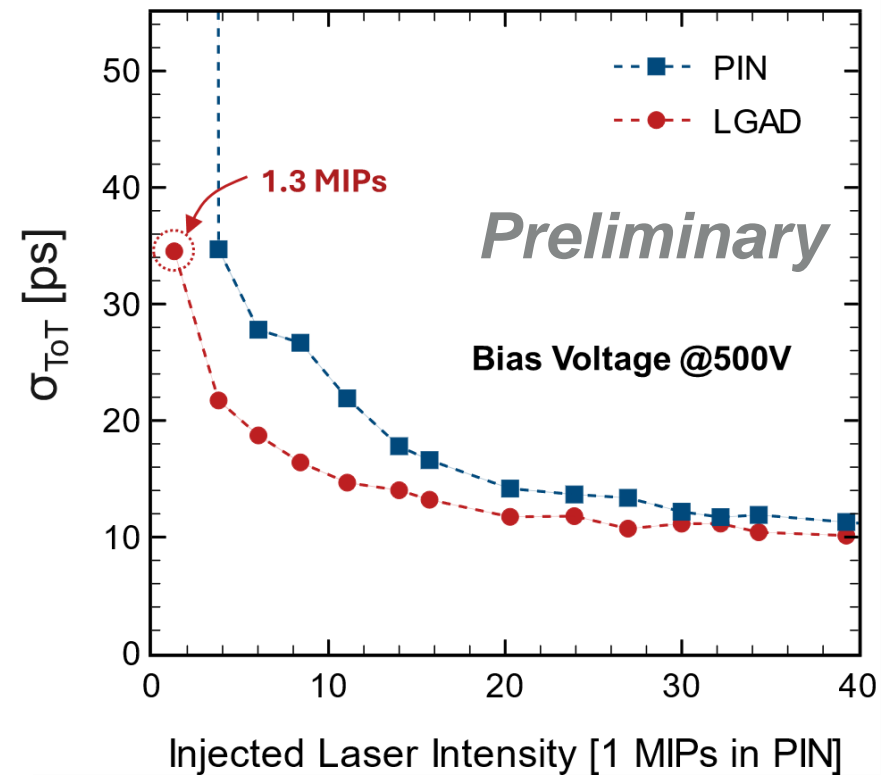
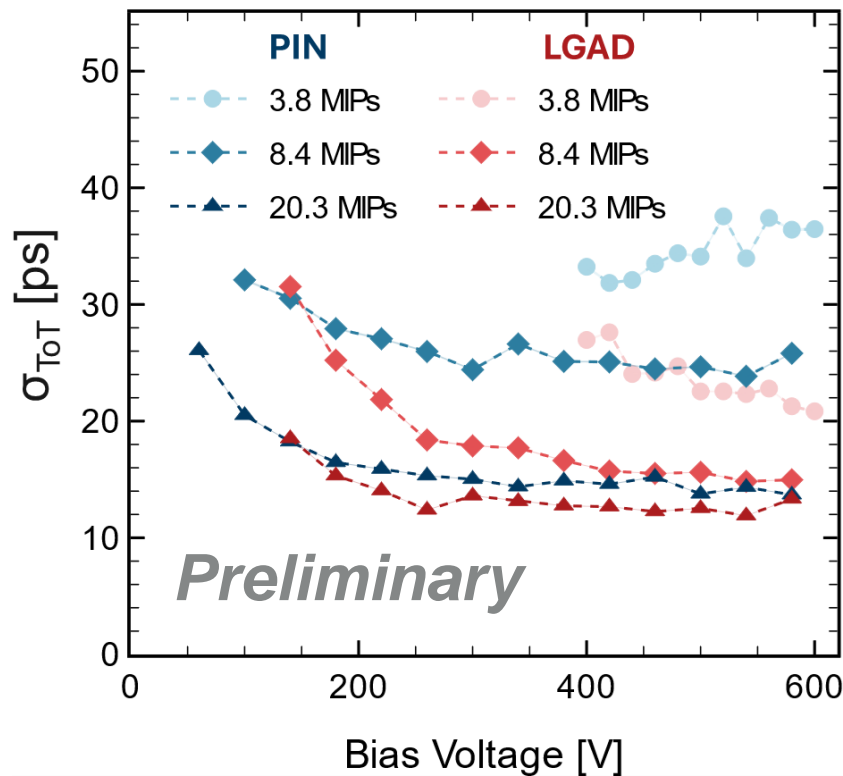
- **Amplitude:** the maximum peak value of signal pulse.
- **Rise Time:** the time interval from 10% to 90% of amplitude.
- **Integration:** the time integral of the pulse signal from TIA.

- **Max Amplitude:** the maximum amplitude in four AC-PADs.
- **Rise Time:** the rise time of the signal pulse that the PAD has the maximum amplitude.
- **SUM Amplitude:** the sum of the amplitudes from the four AC-PADs.

Time Resolution of SiC LGAD

- The 4H-SiC LGAD possesses good time resolution **better than 35 ps** by UV-TCT, significantly outperforming the 4H-SiC PIN in measuring single MIP signals.
- The timing resolution of 4H-SiC LGADs at room temperature is already comparable to that of most Si LGADs operating at both room temperature and low temperatures.
- It is expected that designing higher gain devices will help to achieve better time resolution less than 20 ps.

$$\sigma_{ToT}^2 = \sigma_A^2 + \sigma_{Jitter}^2 + \sigma_{Trigger}^2 + \sigma_{TDC}^2 + \sigma_{sensor}^2 + \cancel{\sigma_{MIPs}^2}$$



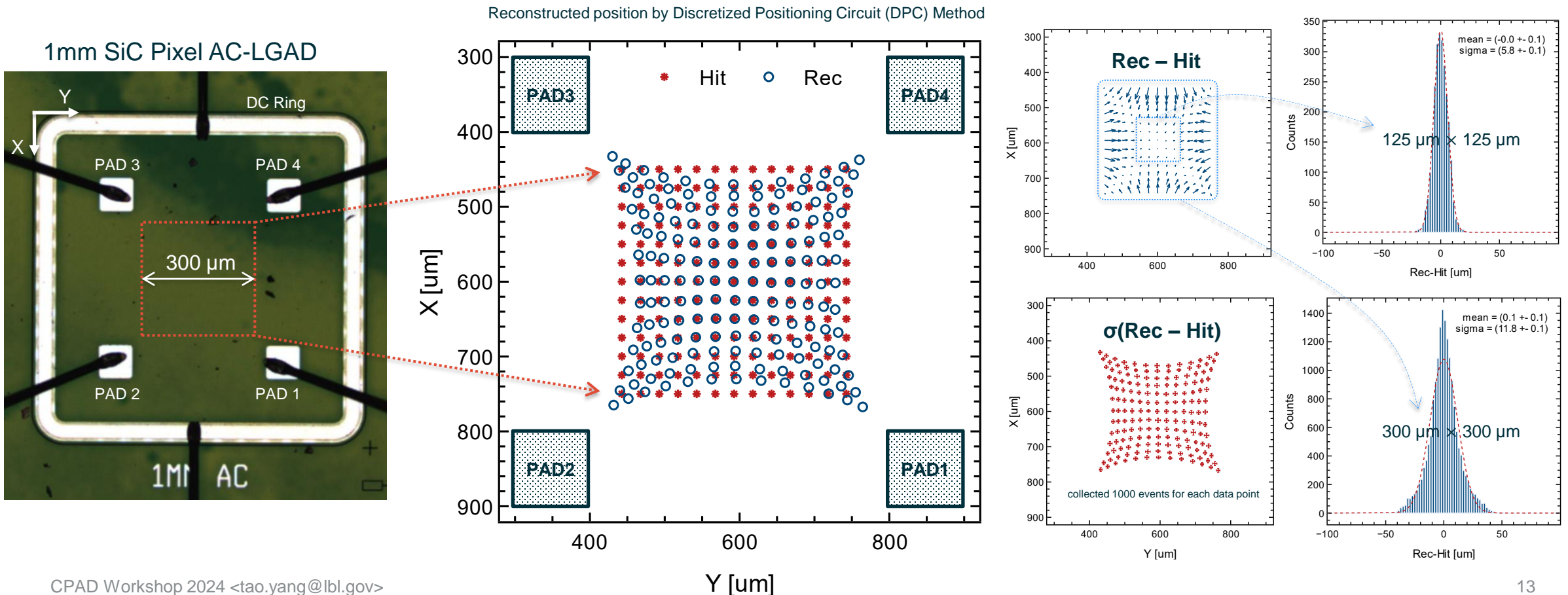
The laser intensity is scaled by the collected charges from the 4H-SiC PIN to match the average charge generated by one MIP in 75 μm of 4H-SiC, which is 4275 e-.

Position Resolution of SiC AC-LGAD

- The SiC AC-LGAD demonstrates good position resolution with $\sigma = 5.8 \mu\text{m}$ in the central region.
- The reconstructed position near the edges currently exhibits distortion due to limitations in the reconstruction algorithm (pad shape and charges leakage by DC-Ring), this issue can be addressed through **algorithm optimization** and **electrode shape optimization**.

$$\sigma_P^2 = \sigma_A^2 + \sigma_{\text{jitter}}^2 + \sigma_{\text{algorithm}}^2 + \sigma_{\text{sensor}}^2 + \cancel{\sigma_{\text{MIPs}}^2}$$

More details will be reported on [2nd CERN DRD3 Workshop](#), December 2nd ~6th, 2024



Conclusion

- TCAD simulations and I-V measurements revealed that the **field plate** effectively mitigates the high electric field induced by the negative bevel-etched angle, greatly increase the breakdown voltage of the 4H-SiC LGAD. This approach can be applied to bevel-etched angles ranging from 1 to 90 degrees.
- By comparing the α particle response of 4H-SiC LGAD and 4H-SiC PIN, we achieved low-gain carrier multiplication in the 4H-SiC LGAD prototype. Observe **larger gain** with **a higher doping concentration** of the gain layer.
- UV-TCT measurements were used to compare the gain and **timing resolution** of the 4H-SiC LGAD and the 4H-SiC PIN, revealing for the first time the outstanding timing capabilities of the 4H-SiC LGAD, with a time resolution **better than 35 ps** for single MIP signals.
- The SiC AC-LGAD demonstrates good **position resolution** with $\sigma = 5.8 \mu\text{m}$ in the central region, but the optimization of reconstruction algorithms and electrode shapes are necessary in the future.

Next

- Initial irradiation using 2.5 GeV protons beam at BNL is completed, the characterization of irradiated devices is in progress.

NASA Space Radiation Laboratory (NSRL)



Radiation Setup at NSRL



- Beam test at SLAC, 70 MeV electron, schedule on January 2025
- Comprehensive study based on 4H-SiC LGADs with different doping and different geometric shapes.
- Further refine device design: ion implantation, new epitaxial wafers (lower doping of drift layer), passivation process and bevel-etching process. The simulation and process validation are in progress by NCSU.

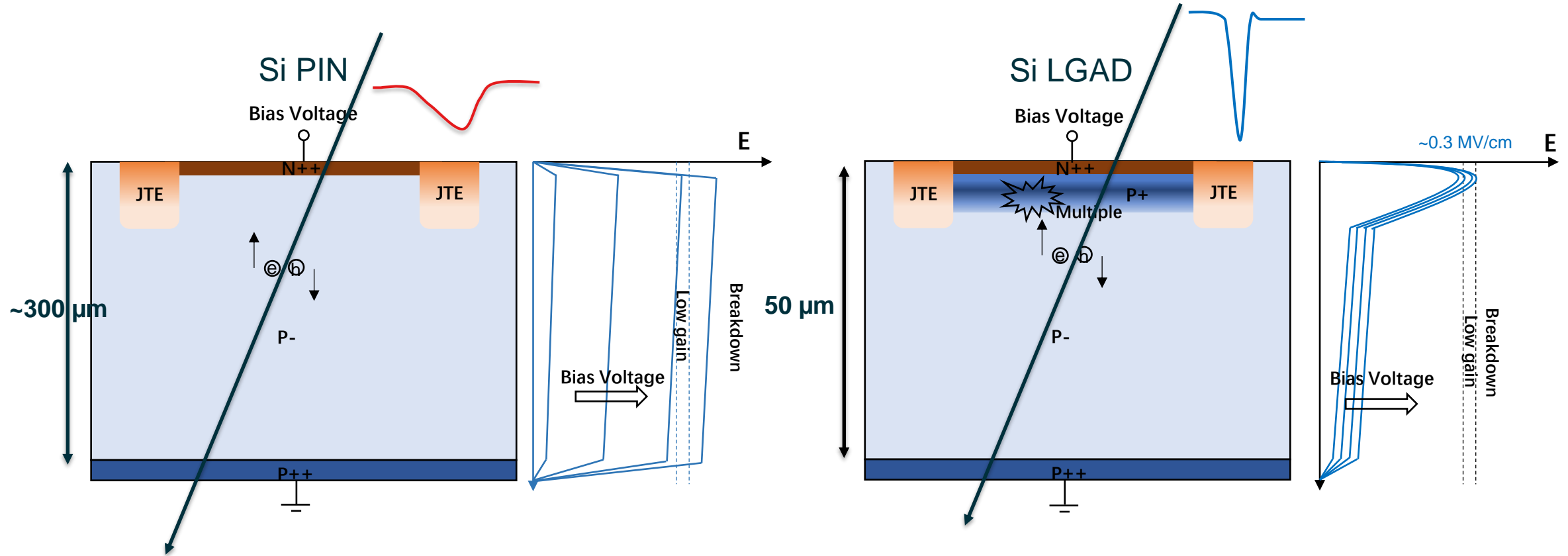
Thanks for your attention

Backup

Silicon Low Gain Avalanche Detector

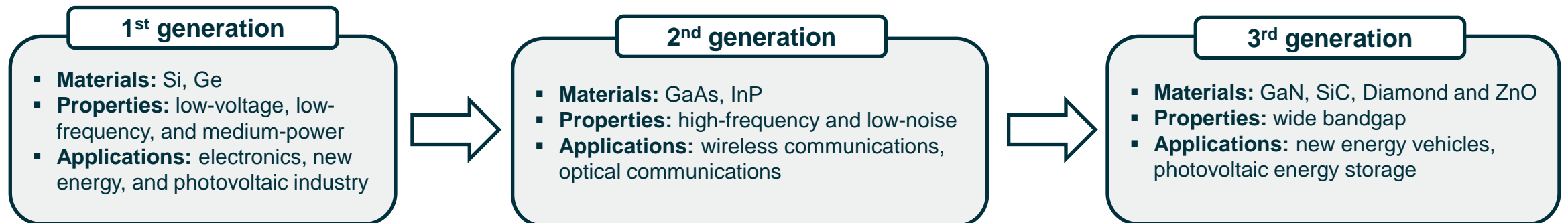
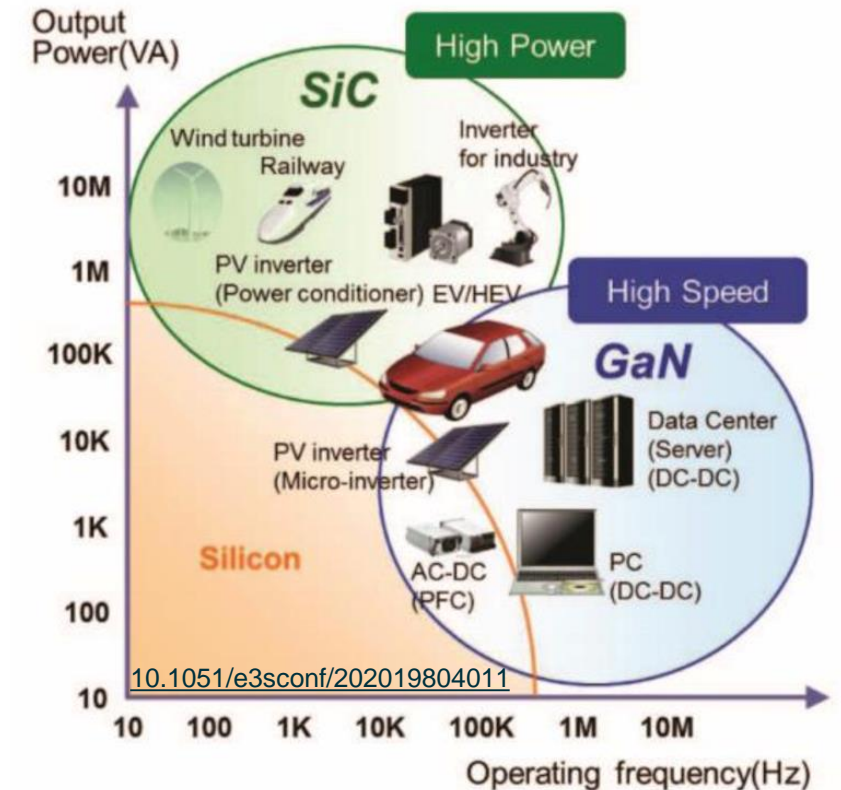
PIN and LGAD

- LGAD has **long operating voltage range with low gain 10~100**.
- The electric field in the gain layer could make carries multiplication but don't reach the breakdown threshold.
- Si LGAD has been characterized by an **excellent timing resolution < 50 ps** benefited its great S/N.



Third generation (Wide Bandgap) Semiconductors

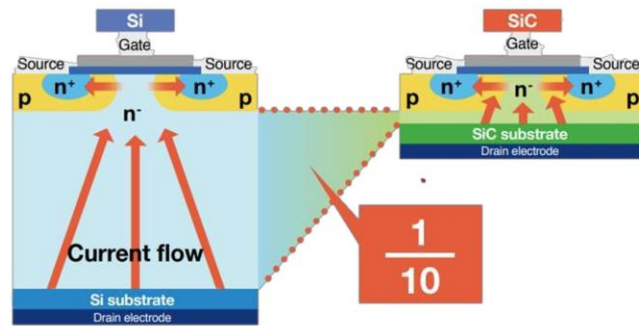
- **First generation semiconductors (indirect bandgap & narrow bandgap)** : Since 1950, semiconductor materials represented by silicon (**Si**) have replaced electron tubes, which is suitable for **low-voltage, low-frequency, and medium-power** integrated circuits.
- **Second-generation semiconductors (direct bandgap & narrow bandgap)** : Since 1990, such as gallium arsenide (**GaAs**), indium phosphide (**InP**). They are suitable for making **high-speed, high-frequency, high-power and light-emitting electronic devices**.
- **Third generation semiconductors (direct bandgap & wide bandgap)** : long history but limited by process technologies. In recent years, materials represented by gallium nitride (**GaN**) and silicon carbide (**SiC**) have attracted much attention with the development of process technologies, which are suitable for making **high temperature, high frequency and high power devices**.



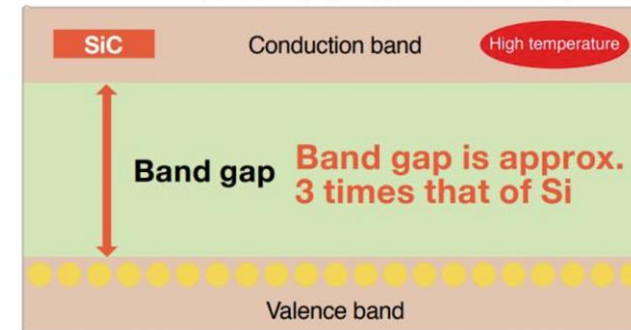
Silicon Carbide(SiC) for Integrated Circuit

Silicon Carbide is useful for power devices and high-speed switching.

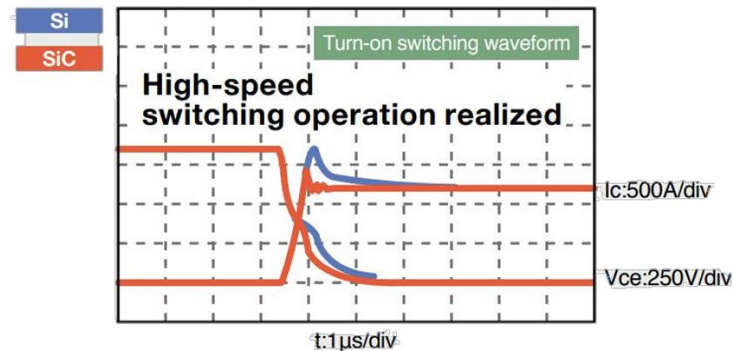
- **Low power consumption:** On-resistance of SiC device is only 1/10 of that of Si



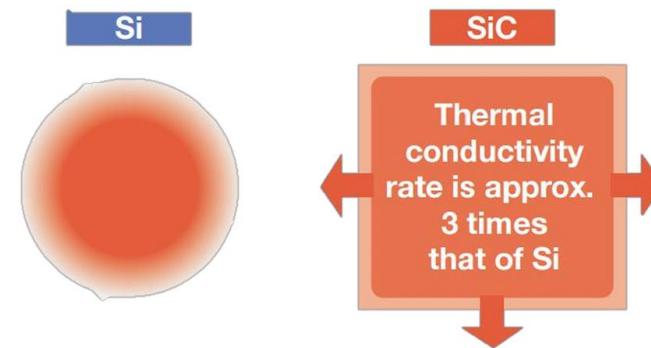
- **High temperature resistance:** SiC's bandgap is three times that of Si, preventing leakage current flow and allowing operation at high temperatures.



- **High-speed switching:** high drift velocity and small transit time



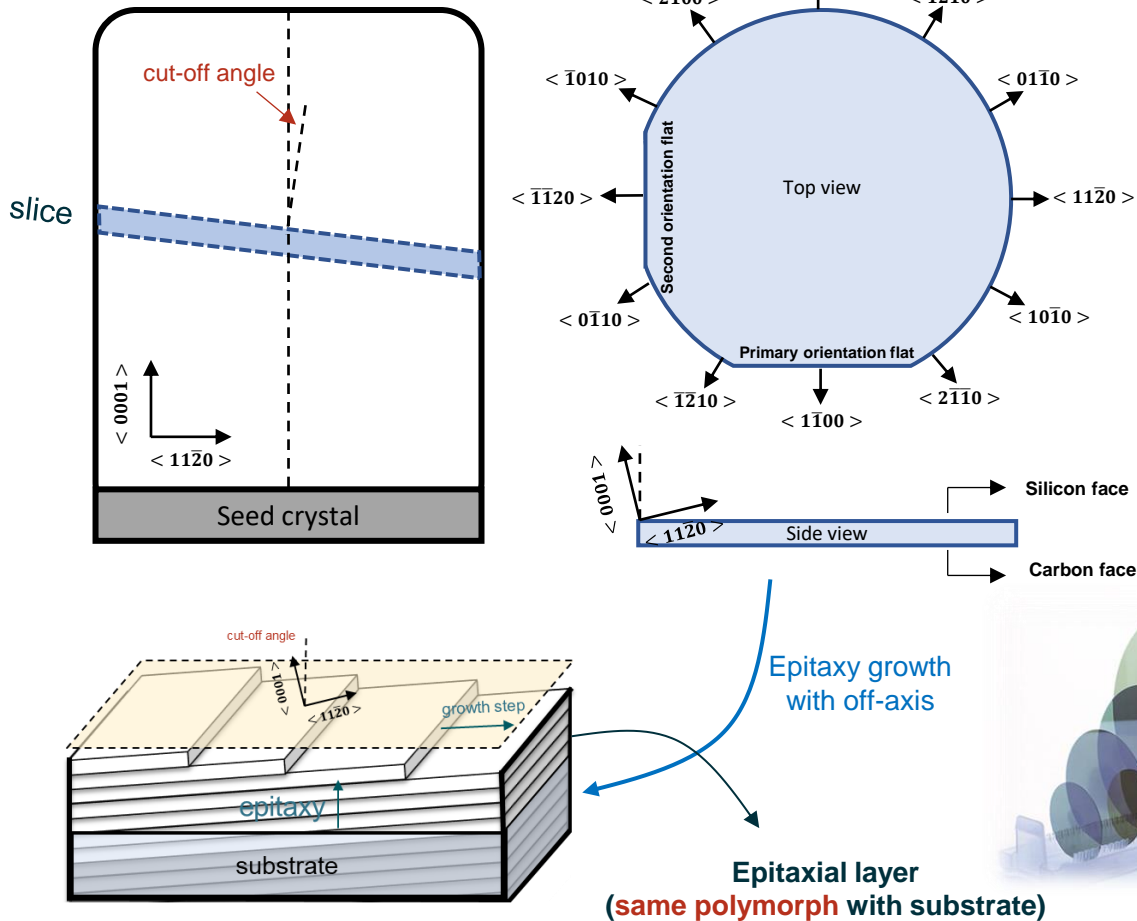
- **Heat dissipation:** the thermal conductivity of SiC is about 3 times that of Si, which dissipates heat quickly.



Epitaxial Growth of Silicon Carbide

Silicon Carbide has had a long history, but for many years was limited by crystal quality including micropipes and basal plane defects. Schottky Barrier Diodes were first made widely available in the early 2000's followed by the commercialization of high voltage MOSFETS around 2011.

SiC Wafer and Epitaxial Growth



- Benefiting from **off-axis** epitaxial growth technology, which provides high purity, good doping control and uniformity, SiC became the preferred choice for power device fabrication in the mid-1990s.
- Currently there are several vendors offering SiC epitaxy and wafers, with the number of wafers produced per year growing rapidly as SiC is adopted to replace silicon in power electronics.

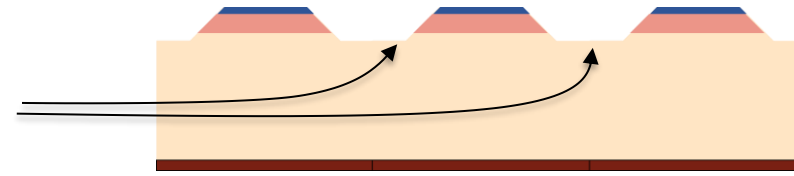
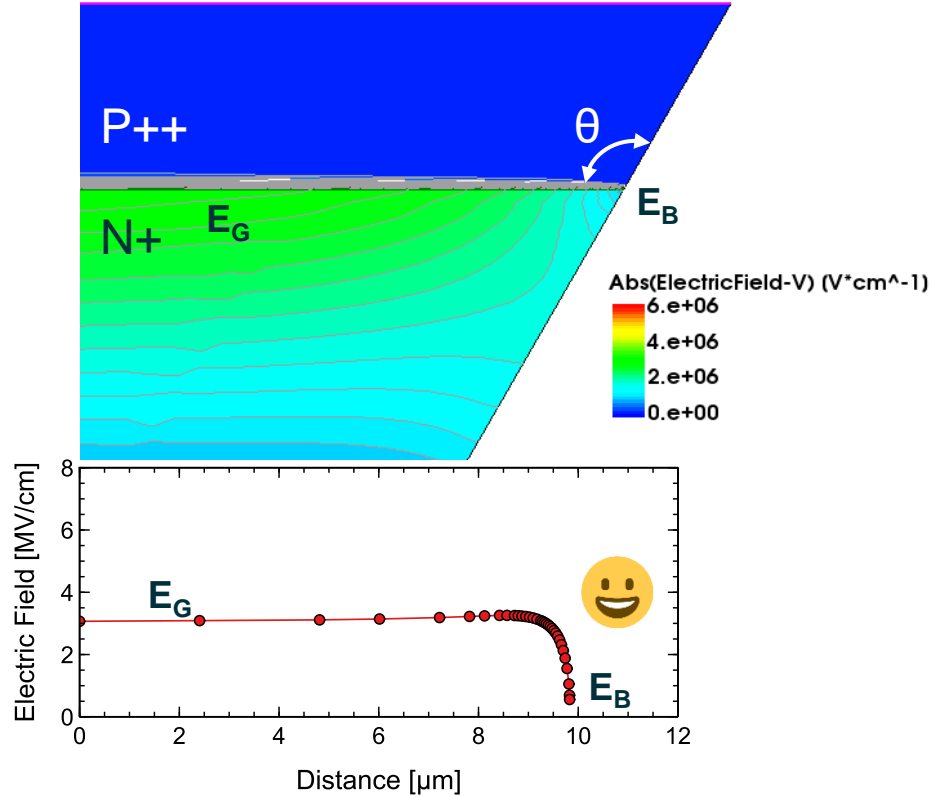
- wafer size: 3 / 4 / 6 / 8 inch
- epi thickness: <math>< 200 \mu\text{m}</math>
- epi doping range: $1\text{e}14 \sim 2\text{e}19 \text{ cm}^{-3}$

The image displays logos for several major vendors in the Silicon Carbide (SiC) industry. The vendors shown are: Wolfspeed, COHERENT, I-III, NOVA SiC, CREE, TYSiC, 天域 TIANYU, SUMITOMO ELECTRIC, infineon, ROHM SEMICONDUCTOR, and 瀚天天成 电子科技有限公司.

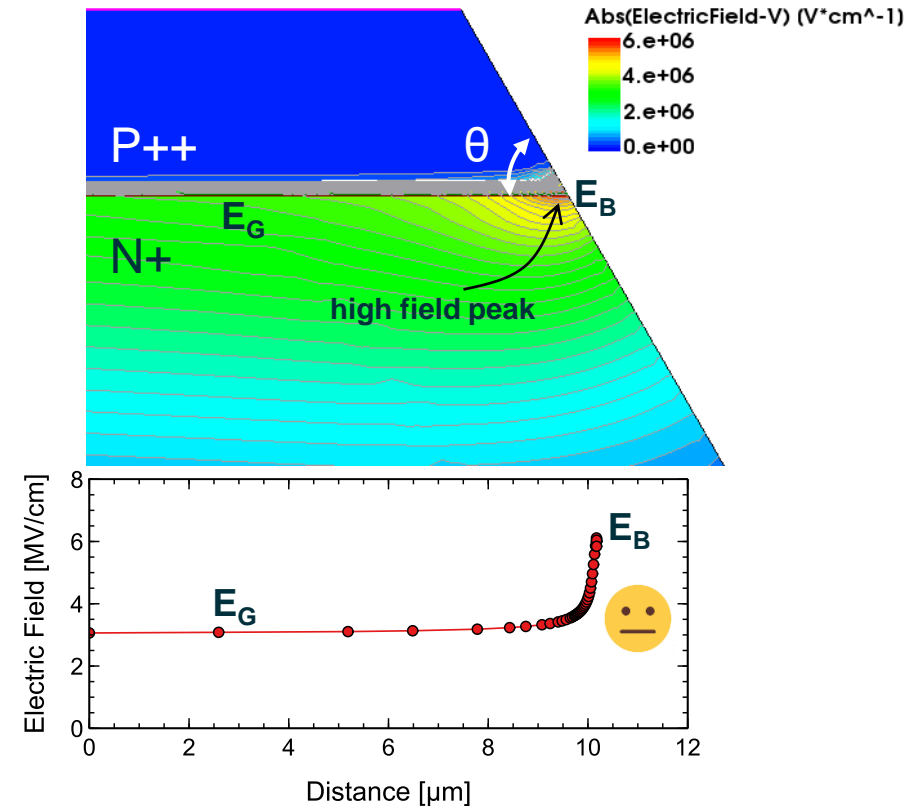
Bevel Termination

Etched bevel termination for device isolation

- **Positive bevel ($\theta > 90^\circ$) :**
more material is removed from the highly doped side to the lightly doped side of the PN junction.

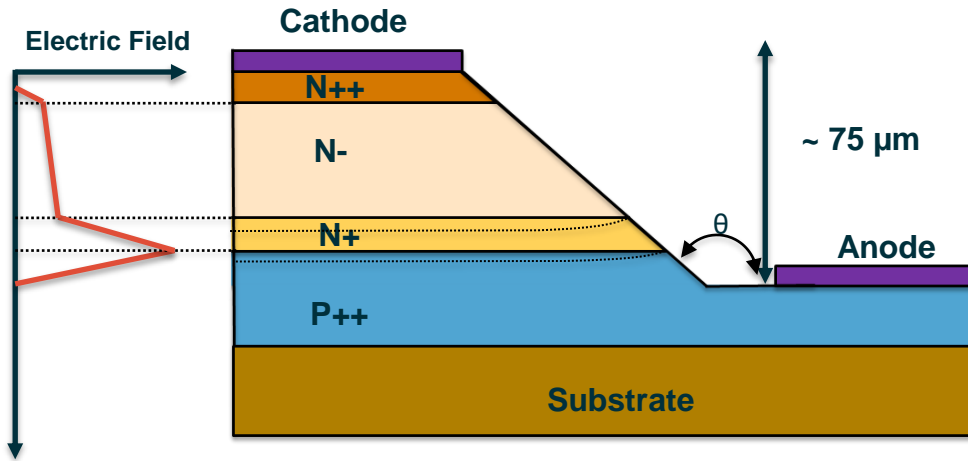


- **Negative bevel ($\theta < 90^\circ$) :**
less material is removed from the highly doped side to the lightly doped side of the PN junction.



SiC LGAD with Bevel Termination

- Ideal SiC LGAD with positive bevel termination



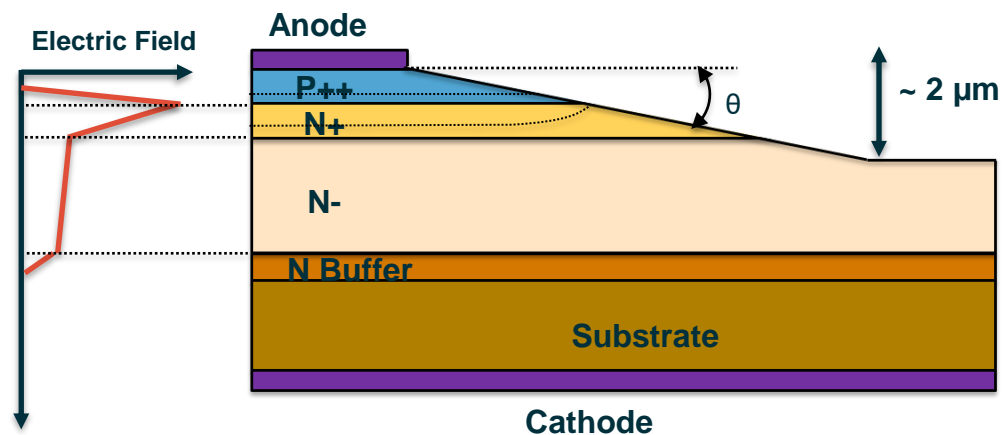
Feature:

Positive bevel termination with maximizing the breakdown voltage.

Difficulty:

Difficult to achieve $\sim 75 \mu\text{m}$ bevel etch with existing technology.

- Realizable SiC LGAD with negative bevel termination



Feature:

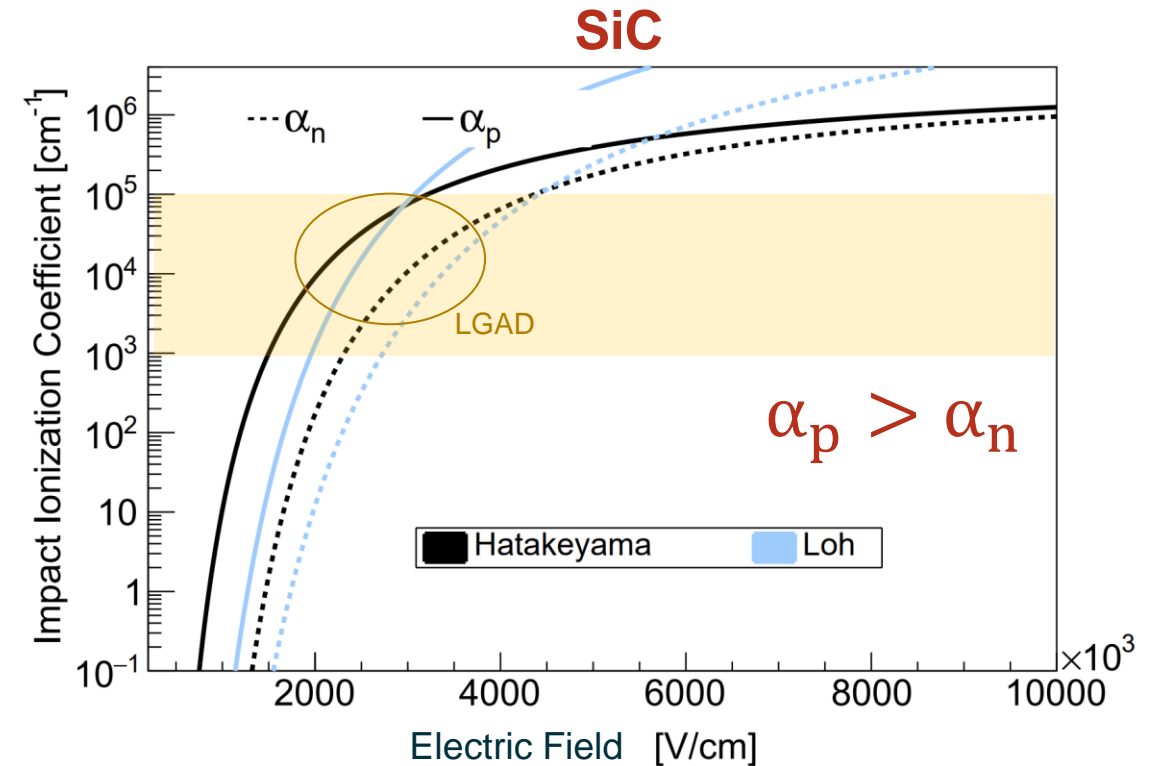
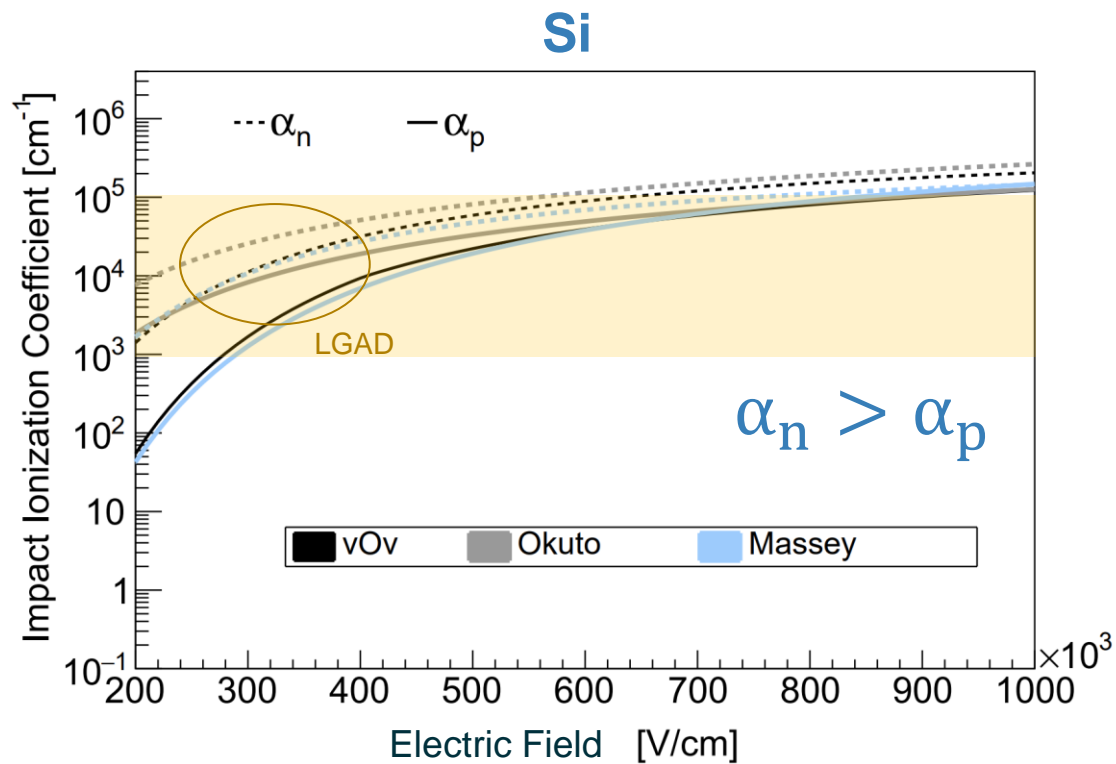
Could achieve $\sim 2 \mu\text{m}$ bevel etching with existing technology.

Difficulty:

The electric field at the bevel surface will be larger than the field in the bulk. It is easy to cause early breakdown of the device.

Impact ionization coefficient $\alpha_{Si} > \alpha_{SiC}$

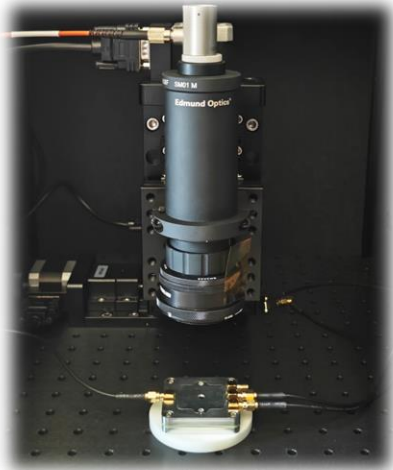
- In silicon carbide, it has smaller impact ionization coefficient than silicon at the same electric field. And the holes has larger impact ionization coefficient. Thus, the SiC LGAD should be designed with **N-type drift layer** and higher electric field (Si: ~ 0.3 MV/cm ; SiC: ~ 3 MV/cm).



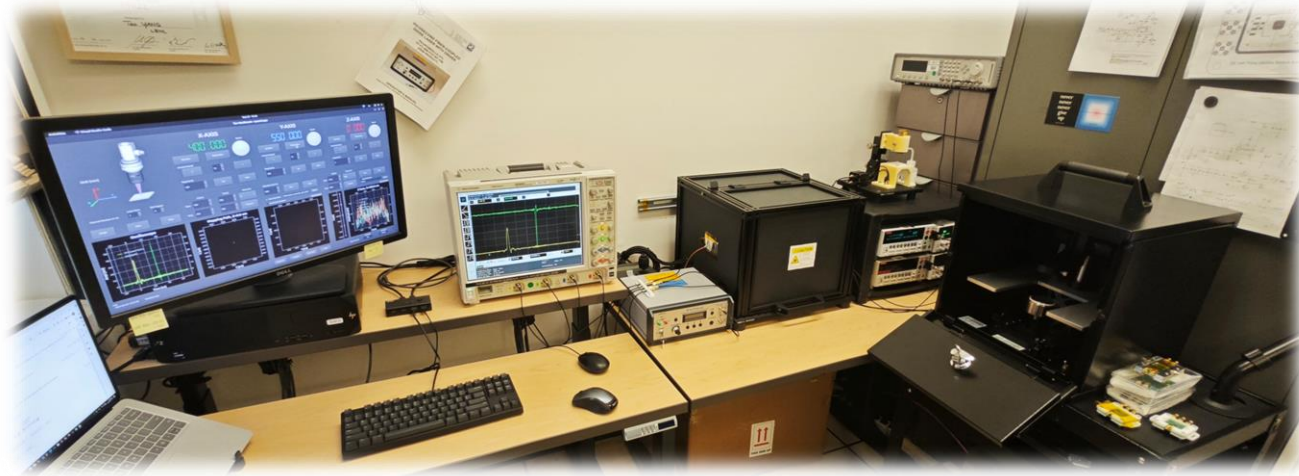
SiC Detector Test Setup of LBNL

Supported by LBNL Physics Division Detector R&D program (KA25)

- UV-TCT Setup



- SiC detector test workbench



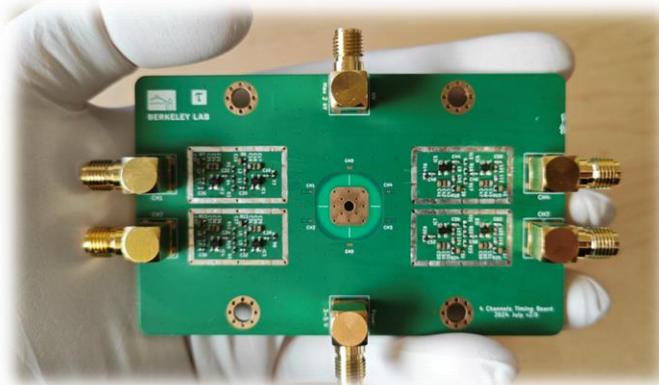
- HV probe station



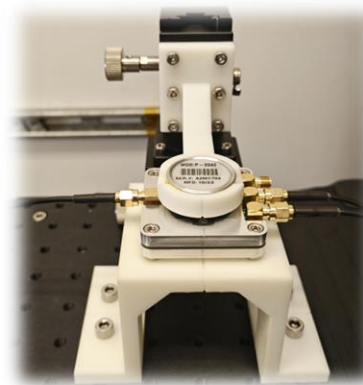
- Single channel TIA board



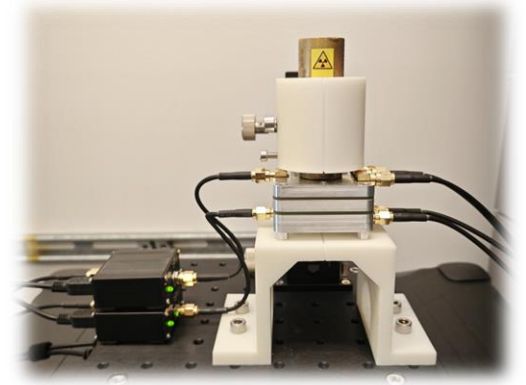
- Four channels TIA board



- α source test setup



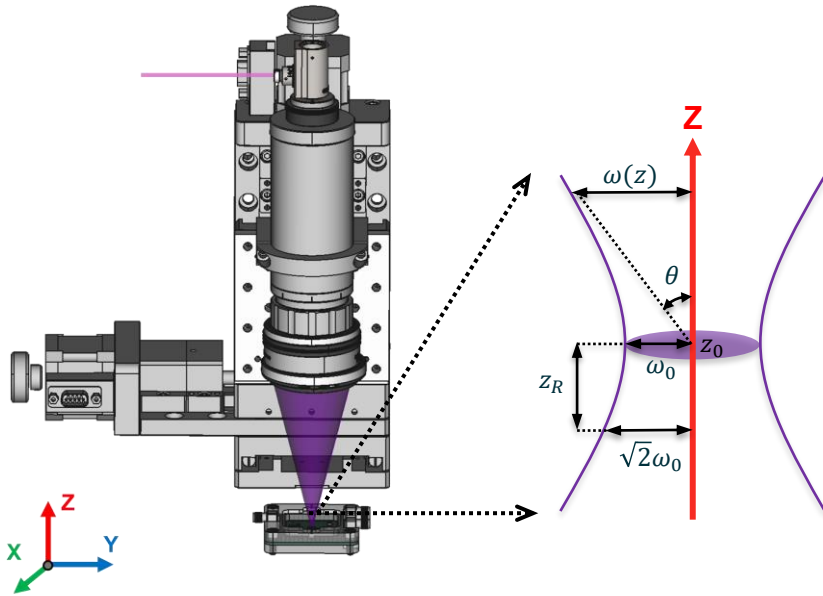
- β source test setup



LaserScope GUI for UV-TCT

The screenshot displays the 'Tao Workbench - LaserScope' interface. At the top left is a 3D schematic of the probe head with a coordinate system (X, Y, Z) and a 'Unit [um]' label. The main control area is divided into three columns for X, Y, and Z axes. Each column has a digital display for position, a speed dial (set to 2048), 'Set Zero' and 'Reset Zero' buttons, an 'Increment [um]' section with left/right arrows and a '10' value, and a 'Target [um]' section with a 'Go' and 'Stop' button. The X-axis target is 600, the Y-axis target is 370, and the Z-axis target is 0. Below these are control buttons for 'Laser Sync' (0), 'DUT Signal' (1), and 'Show Max Ampl' (checked). There are 'Single', 'Auto', and 'Stop' buttons. The bottom row contains four plots: 1. 'Oscilloscope' showing amplitude [mV] vs time [ns] for four channels (CH1-4). 2. 'Mapping Path, Z=0.0 um' showing a square path on an X-Y plane. 3. A grayscale image of a device structure. 4. 'Z Scan, X=600.0 um' showing amplitude [mV] vs Y [um] for a Z=0.0 um scan. At the bottom, there are buttons for 'Amplitude', 'Integral', 'Rise time', 'SNR', and 'Best Focus Z' (set to None).

Characterization of the Laser Beam Profile



Based on the TEM₀₀ Gaussian mode, the intensity distribution of a Gaussian beam:

$$I(r, z) = I_0 \frac{\omega_0^2}{\omega^2(z)} \exp\left(-\frac{2r^2}{\omega^2(z)}\right) \quad \omega(z) = \omega_0 \sqrt{1 + \left(\frac{z - z_0}{z_R}\right)^2}$$

where r is the radial coordinate and I_0 defines the intensity in the center of the beam focus. $\omega(z)$ describes the dependency of the width of the laser beam on the z -position. The spot size has a minimum at $z = z_0$, z_R is the Rayleigh length.

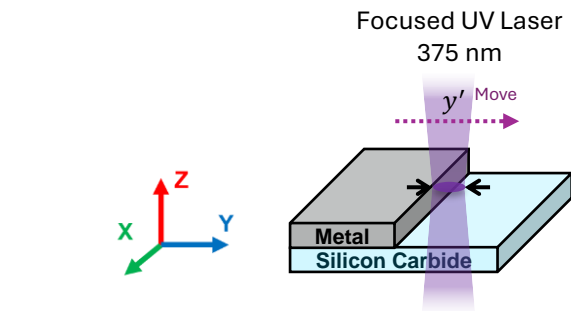
For the laser beam is moved into the metal edge on the y -direction, if the metal edge at $y = 0$, the measured intensity I_m when the laser beam at y' is

$$I_m(y', z) = \int_{y'}^{+\infty} dy \int_{-\infty}^{+\infty} I(x, y, z) dx = I_0 \frac{\omega_0^2}{\omega^2(z)} \int_{y'}^{+\infty} dy \int_{-\infty}^{+\infty} \exp\left(-\frac{2(x^2 + y^2)}{\omega^2(z)}\right) dx$$



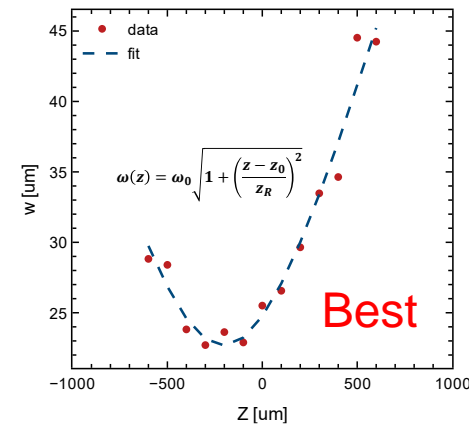
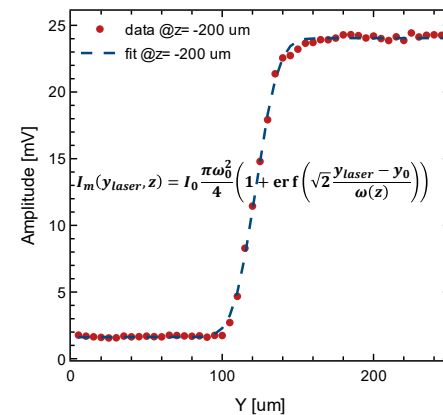
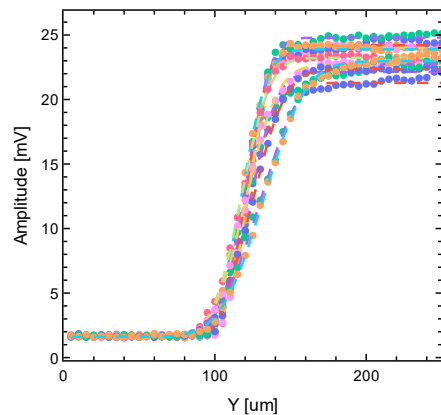
$$I_m(y_{laser}, z) = I_0 \frac{\pi \omega_0^2}{4} \left(1 + \operatorname{erf}\left(\sqrt{2} \frac{y_{laser} - y_0}{\omega(z)}\right)\right)$$

where y_{laser} is the position of laser beam and y_0 is the position of the metal edge.

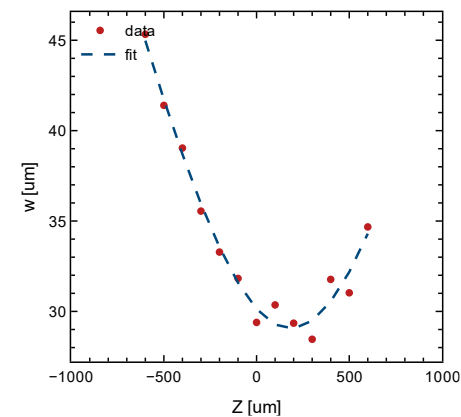
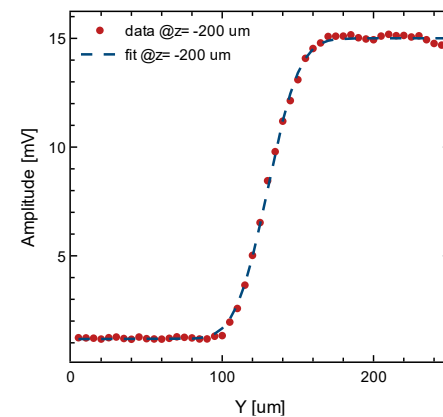
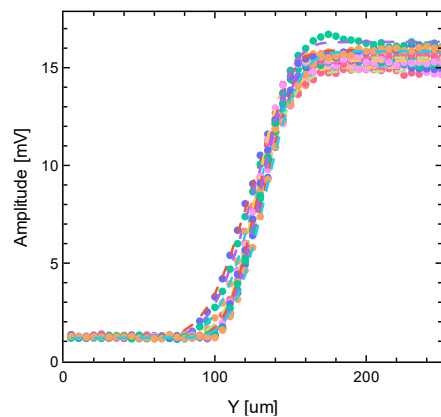


Laser Beam Profile by different lens

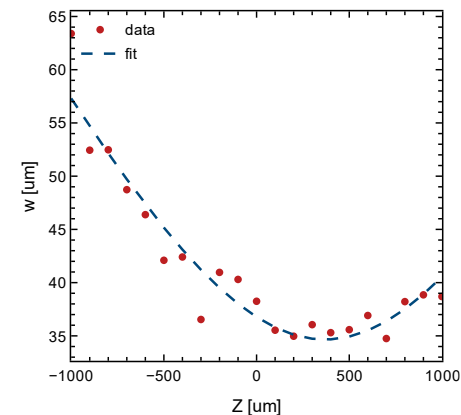
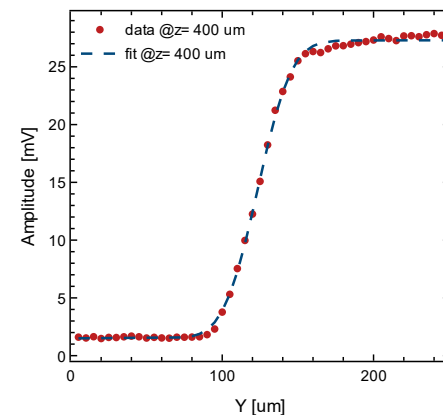
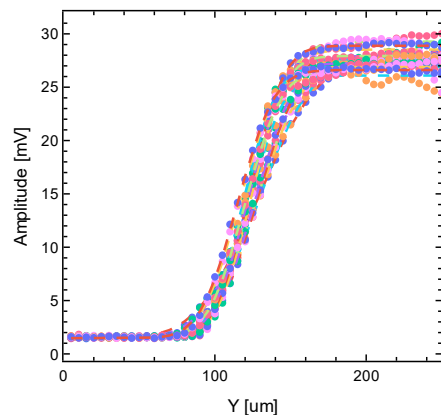
Plano-Convex
 Ø2", f = 60 mm



Achromatic Doublets
 Ø2", f = 75 mm



Plano-Convex
 Ø2", f = 100 mm



Contributions of Time Resolution by UV-TCT

$$\sigma_{TOT}^2 = \sigma_A^2 + \sigma_{Jitter}^2 + \sigma_{Trigger}^2 + \sigma_{TDC}^2 + \sigma_{sensor}^2$$

σ_A^2 is primarily dominated by time walk, which is mainly caused by variations in the energy deposition (such as laser energy consistency and the randomness of avalanche multiplication). This effect can be largely mitigated by using a Constant Fraction Discriminator (CFD).

σ_{Jitter}^2 is dominated by the signal-to-noise ratio (SNR), where $\sigma_{Jitter} = \frac{T_{Rise}}{SNR}$

$\sigma_{Trigger}^2$ is dominated by laser sync trigger pulse which is constant. $\sigma_{Trigger} = 7.7 \text{ ps}$

σ_{TDC}^2 is dominated by sampling rate which is constant. For 20 GSa/s $\sigma_{TDC} = \frac{\Delta T}{\sqrt{12}} = 14.4 \text{ ps}$

σ_{sensor}^2 is dominated by electric field uniformity, device structure, ...

Laser sync trigger pulse

$$\sigma_{\text{Trigger}} = \sqrt{\frac{\sigma^2(T_{\text{post-pulse}} - T_{\text{pre-pulse}})}{2}} = 7.7 \text{ ps}$$

